

# Causal structure of acoustic spacetimes

Carlos Barceló <sup>\*</sup>, Stefano Liberati <sup>†</sup>, Sebastiano Sonego <sup>‡</sup>, and Matt Visser <sup>§</sup>

<sup>\*</sup>*Instituto de Astrofísica de Andalucía (CSIC), Camino Bajo de Huétor 24, 18008 Granada, Spain*

<sup>†</sup>*International School for Advanced Studies (SISSA), Via Beirut 2-4, 34013 Trieste, Italy  
and INFN, Trieste, Italy*

<sup>‡</sup>*Università di Udine, Via delle Scienze 208, 33100 Udine, Italy*

<sup>§</sup>*School of Mathematical and Computing Sciences, Victoria University of Wellington, New Zealand*

8 August 2004; V2: 1 Sept 2004; L<sup>A</sup>T<sub>E</sub>X-ed November 2, 2018; gr-qc/0408022

## Abstract

The so-called “analogue models of general relativity” provide a number of specific physical systems, well outside the traditional realm of general relativity, that nevertheless are well-described by the differential geometry of curved spacetime. Specifically, the propagation of acoustic disturbances in moving fluids are described by “effective metrics” that carry with them notions of “causal structure” as determined by an exchange of sound signals. These acoustic causal structures serve as specific examples of what can be done in the presence of a Lorentzian metric without having recourse to the Einstein equations of general relativity. (After all, the underlying fluid mechanics is governed by the equations of traditional hydrodynamics, not by the Einstein equations.) In this article we take a careful look at what can be said about the causal structure of acoustic spacetimes, focusing on those containing sonic points or horizons, both with a view to seeing what is different from standard general relativity, and to seeing what the similarities might be.

PACS: 02.40.Ma, 04.20.Cv, 04.20.Gz, 04.70.-s

Keywords: analogue models, acoustic spacetime, causal structure, conformal structure, Penrose–Carter diagrams.

---

<sup>\*</sup>carlos@iaa.es

<sup>†</sup>liberati@sissa.it; <http://www.sissa.it/~liberati>

<sup>‡</sup>sebastiano.sonego@uniud.it

<sup>§</sup>matt.visser@mcs.vuw.ac.nz; <http://www.mcs.vuw.ac.nz/~visser>

# 1 Introduction

Acoustic spacetimes are curved Lorentzian manifolds that are used to describe the propagation of sound in moving fluids [1, 2, 3, 4, 5, 6]. As such they are equipped with a Lorentzian spacetime metric (strictly speaking, a pseudo-metric) that is associated with the “sound cones” emanating from each event in the spacetime. Though the acoustic spacetimes are in general curved manifolds, with nonzero Riemann tensor, their curvature and evolution (their geometrodynamics) are not determined by the Einstein equations, but are instead implicit in the equations of traditional fluid mechanics [3, 5, 6]. The acoustic effective geometry must not be confused with the “real” spacetime geometry. Indeed, the “real” physical spacetime structure that we experience in a condensed matter laboratory is approximately Minkowskian. Moreover, under normal circumstances the velocities involved are so small in comparison with the velocity of light that we can perfectly well assume that the system is non-relativistic (Galilean), be it classical or quantum.

Because of these features, the acoustic spacetimes play a rather special role with respect to traditional general relativity. They are examples of Lorentzian manifolds without “gravity” and their existence forces us to think deeply and carefully about the distinction between kinematics and dynamics in general relativity — specifically how much of standard general relativity depends on the Einstein equations and how much of it depends on more general considerations that continue to hold independently of the Einstein equations? In particular, this forces us to think about the deep connections and fundamental differences between Lorentzian geometry, the Einstein equivalence principle, and full general relativity. Some features that one normally thinks of as intrinsically aspects of gravity, both at the classical and semiclassical levels (such as horizons and Hawking radiation), can in the context of acoustic manifolds be instead seen to be rather generic features of curved spacetimes and quantum field theory in curved spacetimes, that have nothing to do with gravity *per se* [1, 5, 7, 8].

In this article we will develop an entire bestiary of (1+1)-dimensional acoustic geometries, specifically chosen because of their naturalness from the point of view of flowing fluids. We will focus on the particularly interesting cases in which the acoustic geometries possess one or two sonic points. These geometries will be the starting point of a follow-up paper in which we will investigate their different effects in terms of curved-space quantum field theoretic vacuum polarization.

After describing each of these geometries, we will investigate their global causal structure by the use of Carter–Penrose diagrams. These diagrams make it clear that because the acoustic geometries are not governed by the Einstein equations, their causal structure can be quite different from what is usually encountered in the context of general relativity. In this context, we will also discuss the notion of “maximal analytic extension” in these acoustic geometries on both mathematical and physical grounds. While mathematically the notion of analytic extension makes perfectly good sense, there are now good physical reasons for being cautious. This *may* have implications for physical gravity and in particular for the ability to characterize spacetime structure by a single well-behaved metric (as opposed to a multi-metric theory). Since this is the first step towards implementing any version of the equivalence principle, it strikes at the very foundations of general relativity.

The geometrical analyses of acoustic spacetimes we are going to present are also interesting for two additional reasons:

1. Because we have a very specific and concrete physical picture for these acoustic

spacetimes it is sometimes easier for a classically trained physicist to see what is going on, and to then use this as a starting point for investigations of the perhaps more formal causal structure in standard general relativity.

2. Conversely, relativists can adopt their training to ask questions in acoustics that might not normally occur to classically trained acoustic physicists.

After dealing with some fundamental issues in section 2 we shall introduce the concept of null coordinates in section 3. In section 4 we develop a “zoo” of stationary acoustic spacetimes, focussing on situations with either one or two sonic points. Section 5 looks at the dynamical evolution of acoustic horizons as the fluid flow is switched on from zero flow to the fully developed flows considered in section 4. In sections 6 and 7 we investigate the global causal structure of the stationary and dynamical acoustic spacetimes by the use of Penrose–Carter diagrams, while the mathematical possibility of performing an analytical extension for acoustic spacetimes will be considered and discussed in section 8. Finally, our summary and conclusions are presented in section 9.

## 2 Fundamental features

We start by pointing out that in acoustic spacetimes, as in general relativity, causal structure can be characterized in two complementary ways — in terms of the rays of geometrical acoustics/optics or in terms of the characteristics of the partial differential equations (wave equations) of physical acoustics/optics [6, 9].

At the level of geometrical acoustics we need only assume that:

- the speed of sound  $c$ , relative to the fluid, is well defined;
- the velocity of the fluid  $\vec{v}$ , relative to the laboratory, is well defined.

Then, relative to the laboratory, the velocity of a sound ray propagating, with respect to the fluid, along the direction defined by the unit vector  $\vec{n}$  is

$$\frac{d\vec{x}}{dt} = c\vec{n} + \vec{v}, \quad (2.1)$$

which defines a sound cone in spacetime given by the condition  $\vec{n}^2 = 1$ , i.e.,

$$-c^2 dt^2 + (d\vec{x} - \vec{v} dt)^2 = 0. \quad (2.2)$$

This is associated with a conformal class of Lorentzian metrics [5, 6]

$$g = \Omega^2 \left[ \begin{array}{c|c} -(c^2 - v^2) & -\vec{v}^T \\ \hline -\vec{v} & \mathbf{I} \end{array} \right], \quad (2.3)$$

where  $\Omega$  is an unspecified non-vanishing function. The virtues of the geometric approach are its extreme simplicity and the fact that the basic structure is dimension-independent.

At the level of physical acoustics, setting up an acoustic spacetime is a little trickier. For technical reasons it is easiest to confine attention to an irrotational flow for a fluid

with a barotropic equation of state, in which case it is relatively straightforward to derive, in any number of dimensions, a wave equation of the form [5, 6]

$$\partial_a (f^{ab} \partial_b \theta) = 0 . \quad (2.4)$$

Turning this into a statement about a metric requires the identification

$$(-\det g)^{1/2} g^{ab} = f^{ab} , \quad (2.5)$$

where, as usual,  $g$  denotes the matrix  $[g_{ab}]$ , obtained by inverting  $g^{-1} \equiv [g^{ab}]$ . Defining now  $\det f = 1/\det[f^{ab}]$  we have

$$-\det g = (-\det f)^{-2/(d-2)} , \quad (2.6)$$

and

$$g^{ab} = (-\det f)^{1/(d-2)} f^{ab} . \quad (2.7)$$

With this procedure one gets, for a fluid with mass density  $\rho$ , a metric of the form (2.3), with  $\Omega^2$  equal to an unspecified positive constant multiplied by some power of  $\rho/c$ .

However, the exponent in equation (2.7) indicates that  $g^{ab}$  and  $g_{ab}$  are not defined in  $d = 2$  (that is, in 1+1 dimensions). Fortunately this problem is formal rather than fundamental. One can always augment any interesting (1+1)-dimensional acoustic geometry by two extra flat space dimensions — which is after all exactly how such a geometry would actually be experimentally realised, letting the fluid flow along a thin pipe — and simply phrase physical questions in terms of the plane symmetric 3+1 geometry. Alternatively, one could forget the extra dimensions and simply ask questions based on the geometric acoustics approximation, which, after all, is quite sufficient for dealing with issues of causal structure.

We mention in passing that attempts to include vorticity into the physical acoustics formalism lead to a more complicated mathematical structure of which the “effective metric” is only one part. Fortunately the eikonal approximation (the geometrical acoustics approximation) again leads to the conformal class of metrics considered above and as far as issues of causal structure are concerned, there is no significant gain in adding vorticity to the mix [10].

Before going further we also mention that for any metric of the form (2.3) we have:

$$g^{-1} = \frac{1}{\Omega^2} \left[ \begin{array}{c|c} -1/c^2 & -\vec{v}^T/c^2 \\ \hline -\vec{v}/c^2 & \mathbf{I} - \vec{v} \otimes \vec{v}^T/c^2 \end{array} \right] . \quad (2.8)$$

Therefore, since

$$g^{-1}(dt, dt) = -1/(c^2\Omega^2) < 0 , \quad (2.9)$$

we see that the natural Newtonian time coordinate provides a “cosmic time” and so the acoustic manifolds are always stably causal [5, 6]. This is one among many special features exhibited by acoustic spacetimes.

In the remainder of this paper we will always consider (1+1)-dimensional acoustic spacetimes and will investigate their causal structure in some detail. From the laboratory point of view, such a spacetime is always a Cartesian product between some open interval  $(t_1, t_2)$  of the real line (time) and some one-dimensional manifold without boundary (space). We shall always consider these spacetimes as eternally existing entities, so that

in effect  $t_1 = -\infty$  and  $t_2 = +\infty$ . It is well-known that any smooth, connected one-dimensional manifold without boundary is diffeomorphic either to  $\mathbb{R}$  or to the circle  $S^1$  [11]. Hence, the only two possible diffeomorphism classes for our acoustic manifolds are either  $\mathcal{M} = \mathbb{R}^2$  or  $\mathcal{M} = \mathbb{R} \times S^1$ . This simple observation already greatly constrains the topology of our acoustic spacetimes. Additionally, on these manifolds there are preferred coordinates, that we denote  $t$  and  $x$ , associated with time and distance readings by means of physical Newtonian clocks and rulers. We have  $t \in \mathbb{R}$ , and  $x \in \mathbb{R}$  or  $x \in (-L, L)$ , according to whether space is topologically a line or a circle. Note that the acoustic spacetimes, armed with such a notion of measurement, are automatically inextensible manifolds for physical reasons.

As we have said before, associated with the irrotational flow of a barotropic, viscosity-free fluid, there is an *acoustic metric* on  $\mathcal{M}$ ,

$$g = \Omega^2 \left[ - (c^2 - v^2) dt^2 - 2v dt dx + dx^2 \right], \quad (2.10)$$

where  $c$  is the speed of sound and  $v$  the fluid velocity [1, 3, 5, 6]. Now in general,  $c$  and  $v$  are functions of  $t$  and  $x$ . Here, we shall in the interests of simplicity assume that  $c$  does not depend on position and time. It is therefore the velocity profile  $v(t, x)$  that contains all the relevant information about the causal structure of the acoustic spacetime  $(\mathcal{M}, g)$ .

The effective metric (2.10) is only experienced by acoustic waves (and phonons) in the fluid. Hypothetical “internal” observers, living in the fluid and able to measure distances and times only by means of acoustic structures, might consider the proper distances associated with this acoustic metric to be the actual physical distances [5, 12], at least for low energies [13]. (An early suggestion somewhat along these lines can be found in reference [14].) In contrast, from the “external” laboratory point of view proper distances in  $(\mathcal{M}, g)$  are meaningless, since it is only  $t$  and  $x$  that have empirical content in terms of external laboratory measurements.

Topologically, the manifold  $\mathcal{M}$  is an open set. As we have already mentioned, from the laboratory point of view it is an inextensible manifold. However, from the point of view of the internal observers this manifold might be extensible for certain particular acoustic configurations. Roughly speaking, this can happen when the proper distance to infinity in the acoustic metric becomes finite. In this paper we will analyze configurations with one or more sonic points, in which these phenomena usually happen. These sonic points are points where  $v(t, x) = \pm c$ , and correspond to the so-called acoustic apparent horizons<sup>1</sup> for the Lorentzian geometry defined on  $\mathcal{M}$  by the metric (2.10). In fact, we shall use the terminology “sonic point” and “apparent horizon” interchangeably. At the sonic points, the coefficient of  $dt^2$  vanishes, whereas the determinant of the metric is everywhere equal to  $-c^2$ , hence regular. This suggests that the coordinates  $t$  and  $x$  are somehow inappropriate to describe sound propagation near the sonic points.

Indeed, as we shall see, although by definition  $t$  and  $x$  cover the whole manifold, the behaviour of null curves in a  $(t, x)$  diagram can be singular at the horizons. Moreover,  $t$  and  $x$  convey a wrong impression of the acoustic causal structure, since they are not everywhere timelike and spacelike coordinates with respect to the acoustic metric.

Our primary goals in this article are to give a clear description of the causal structure of

---

<sup>1</sup>We caution the reader that the relative simplicity of the discussion regarding horizons and sonic points depends to a large extent on the simplification of dealing with 1+1 dimensions. In higher dimensions without planar symmetry one should generically distinguish horizons from ergosurfaces [5].

the most natural acoustic spacetimes with sonic horizons; and to emphasize the similarities with, and differences from, the standard black-hole solutions in standard general relativity.

### 3 Null coordinates

In order to explore the causal structure of  $(\mathcal{M}, g)$ , let us introduce retarded and advanced null coordinates as

$$du := F(t, x) \left( dt - \frac{dx}{c + v(t, x)} \right), \quad (3.1)$$

$$dw := G(t, x) \left( dt + \frac{dx}{c - v(t, x)} \right), \quad (3.2)$$

where  $F$  and  $G$  are suitable integrating factors. In these coordinates, the metric is

$$g = -\frac{\Omega^2}{FG} (c^2 - v^2) du dw. \quad (3.3)$$

Of course, for any stationary flow, in which  $v$  does not depend on  $t$ , we can choose  $F \equiv G \equiv 1$ . Let us consider this case in some detail.

Consider a smooth velocity profile with a sonic point at  $x = x_S$ . Then one can write, for  $x$  sufficiently close to  $x_S$ ,

$$v(x) = \sigma c + \epsilon \kappa (x - x_S) + O\left((x - x_S)^2\right), \quad (3.4)$$

where  $\sigma$  and  $\epsilon$  can take on both the values  $\pm 1$ , and

$$\kappa := \left. \frac{dv}{dx} \right|_{x=x_S} \quad (3.5)$$

is a nonnegative quantity which can be interpreted as the normalized surface gravity [5, 8, 15]. There are now four possibilities depending on the values of  $\sigma$  and  $\epsilon$ :

- (i) At the sonic point  $\sigma = -1$  (left-going flow) and  $\epsilon = 1$ ; this corresponds to a black-hole configuration from the point of view of an observer to the right of  $x_S$ ;
- (ii) At the sonic point  $\sigma = 1$  (right-going flow) and  $\epsilon = -1$ ; to an observer to the right of  $x_S$ , this corresponds to a white-hole configuration;
- (iii) and (iv) correspond, respectively, to mirror symmetric configurations of (i) and (ii) through the point  $x_S$  (right and left are exchanged).

When  $\sigma = -1$ ,  $w$  is regular at  $x = x_S$ , while  $u$  diverges. The asymptotic expressions near the sonic point are

$$\left. \begin{aligned} u &\sim t - \frac{1}{\kappa} \ln |x - x_S| \\ w &\sim t + \frac{x}{2c} \end{aligned} \right\}. \quad (3.6)$$

When  $\sigma = 1$ , it is  $u$  that is regular, while  $w$  diverges. The asymptotic expressions are

$$\left. \begin{aligned} u &\sim t - \frac{x}{2c} \\ w &\sim t + \frac{1}{\kappa} \ln |x - x_S| \end{aligned} \right\}. \quad (3.7)$$

In both cases, the equation  $x = x_S$  defines a null line in spacetime, where either  $u$  or  $w$  tend to  $+\infty$ . Obviously, the null coordinates  $u$  and  $w$  are unsuitable to describe the geometry in the vicinity of the sonic points, as one can see also from the corresponding expression (3.3) of the metric.

For completeness, we mention that the laboratory coordinates  $t$  and  $x$  are not the analogs of the Schwarzschild-like coordinates commonly used when investigating static solutions of Einstein's equations with spherical symmetry. This is obvious if one thinks (i) that the lines  $t = \text{const}$  are not orthogonal, in the acoustic metric (2.10), to the worldlines of static observers located at  $x = \text{const}$ , and (ii) that  $(t, x)$  are well defined across the sonic points, whereas the Schwarzschild coordinate  $t$  is singular on the horizons. In fact, the coordinates  $t$  and  $x$  correspond instead to the so-called Painlevé-Gullstrand coordinates [16]; see also reference [5]. In order to make this point totally clear, let us introduce Schwarzschild-like coordinates on the relevant portion of the acoustic spacetime.

Starting from the null coordinates  $u$  and  $w$  given by equations (3.1) and (3.2), define  $\tau$  and  $\chi$  such that:

$$d\tau = \frac{1}{2} (dw + du) = dt + \frac{v}{c^2 - v^2} dx; \quad (3.8)$$

$$d\chi = \frac{1}{2} (dw - du) = \frac{c}{c^2 - v^2} dx. \quad (3.9)$$

On replacing these expressions into the metric (3.3) we find

$$g = \frac{\Omega^2}{FG} (c^2 - v^2) (-d\tau^2 + d\chi^2) = \frac{\Omega^2}{FG} \left[ -(c^2 - v^2) d\tau^2 + \frac{c^2}{c^2 - v^2} d\chi^2 \right]. \quad (3.10)$$

It is evident that  $\tau$  and  $x$  are now perfect analogs of the Schwarzschild time and radial coordinates. In particular, (i) the lines  $\tau = \text{const}$  are orthogonal to the worldlines of static observers, and (ii) the coordinate  $\tau$  fails to be defined at the sonic points. On the other hand, the coordinate  $\chi$  is the analogue of the radial coordinate used in the so-called optical geometry [17]. It represents spatial distances as measured in terms of the round-trip time of acoustic signals.

## 4 Stationary zoo

In this section we will describe a series of stationary<sup>2</sup> (1+1)-dimensional spacetime geometries that naturally appear in the context of moving fluids. For each of these geometries we will exhibit a representative and simple to manipulate velocity profile  $v(x)$ . Then, we will show the behaviour of right- and left-moving sound rays in these manifolds by drawing lines  $u = \text{const}$  and  $w = \text{const}$  in a  $(t, x)$  diagram (Painlevé-Gullstrand coordinates).

---

<sup>2</sup>We are using “stationary” in the precise technical sense of assuming the existence of a Killing vector that is timelike in the domain of outer communication.

We will postpone to section 6 the detailed description of the conformal structures of these spacetimes, through the inspection of their conformal diagrams. Furthermore, we leave it for section 8 to show that their metric manifold  $(\mathcal{M}, g)$  can be mathematically extended beyond the physical range of the coordinates  $(t, x)$ , and to discuss the physical interpretation of this “maximal analytic extension”. We have also investigated general flows without sonic points, and report that their causal structure (though not necessarily their geometry) is trivial in the sense that the null geodesics (and indeed the Penrose–Carter diagrams) are qualitatively similar to those of ordinary flat Minkowski space.

## 4.1 Flows with one sonic point

Let us start this catalog of configurations by considering those that possess a single sonic point. Since we are at this stage considering stationary spacetimes, the apparent and absolute event horizons will always coincide. Unfortunately the term “event horizon” has now become so overused that it has to a large extent “lost its trademark” and quite often when one encounters discussion of “event horizons” in the literature the phrase is being misused to vaguely refer to some sort of unspecified horizon-like object. We shall try to be more careful and stick to the proper technical meaning. Hereafter, we shall always use the term “event horizon” as a synonym of the “absolute horizon”, that is the boundary of the causal past of a suitable connected component of future null infinity. In 1+1 dimensions without periodic boundary conditions on space there is a definite and unambiguous notion of “left” and “right” so that null infinity (and indeed spacelike infinity) naturally subdivides into at least two disconnected components. The definition of an event horizon is then subordinated to first choosing the disconnected component of null infinity that is of interest. Similar behaviour occurs, for instance, in the maximally extended Reissner–Nordström or Kerr geometries. Whenever it is not mentioned explicitly, we always use the right null infinity  $\mathfrak{S}_{\text{right}}$  in order to define horizons and black (or white) hole regions. That is, we always make reference to observations performed in the asymptotic region  $x \rightarrow +\infty$ .

### 4.1.1 Black hole

Consider a left-going flow, with one subsonic region and one supersonic; with the flow velocity  $v$  being bounded. A velocity profile that is, at the same time, both representative and simple to manipulate is

$$v(x) = -\frac{2c}{\exp(2x/a) + 1}, \quad (4.1)$$

where  $a$  is a positive constant. This is plotted in figure 1 for  $c = 1$ ,  $a = 1$  (a choice of parameters that we shall adopt for all diagrams in the paper).

Right-moving and left-moving sound rays are described by  $u = \text{const}$  and  $w = \text{const}$ , respectively, where:

$$u = t - \frac{x}{c} - \frac{a}{c} \ln |1 - \exp(-2x/a)|; \quad (4.2)$$

$$w = t + \frac{x}{c} + \frac{a}{3c} \ln(1 + 3 \exp(-2x/a)). \quad (4.3)$$



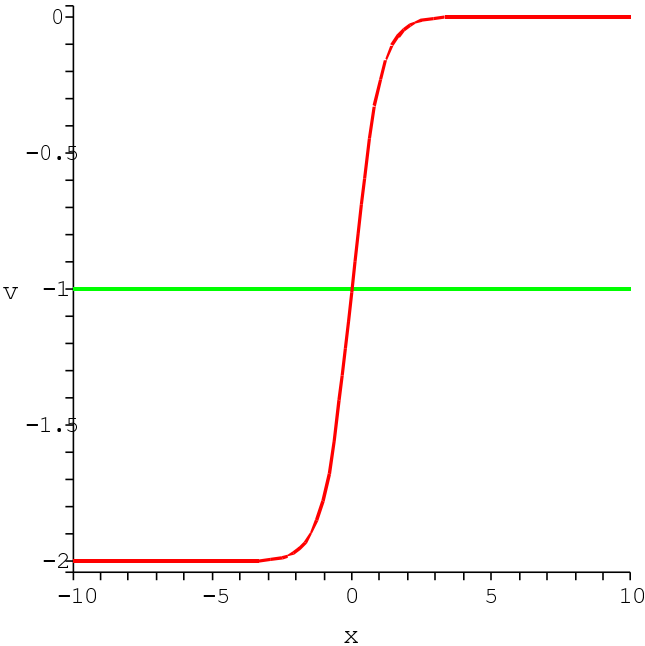


Figure 1: Velocity profile for a left-going flow with one subsonic region ( $x > 0$ ) and one supersonic region ( $x < 0$ );  $v$  bounded: An acoustic black hole.

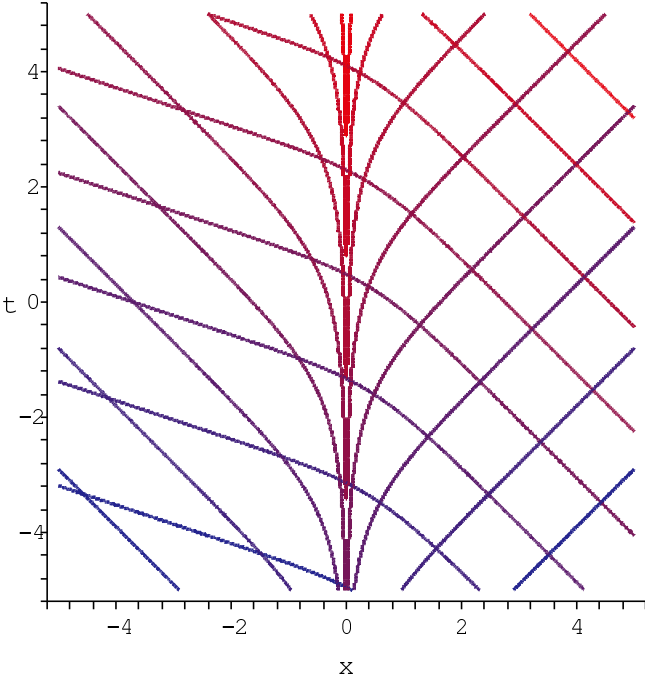


Figure 2: Acoustic black hole. The null curves  $u = \text{const}$  are the blue lines;  $w = \text{const}$  are the red lines.

Figure 2 represents the acoustic spacetime with a few sound rays explicitly shown. The sound rays define the acoustic causal structure. The acoustic horizon is located at  $x = 0$  and the (normalized) surface gravity, defined as we have already mentioned via  $\kappa = |dv/dx|$  evaluated at the apparent horizon, is  $\kappa = c/a$ .

#### 4.1.2 White hole

Consider now a right-going flow, with one subsonic region, and one supersonic; and with  $v$  again bounded. A convenient and easily manipulated example is:

$$v(x) = \frac{2c}{\exp(2x/a) + 1} \quad (4.4)$$

(see figure 3). The null coordinates are

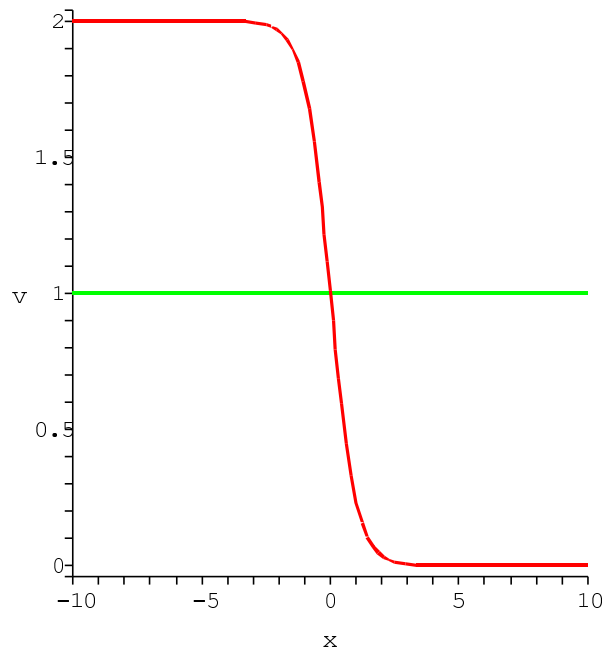


Figure 3: Velocity profile for a right-going flow with one subsonic region and one supersonic region;  $v$  bounded: An acoustic white hole.

$$u = t - \frac{x}{c} - \frac{a}{3c} \ln(1 + 3 \exp(-2x/a)) , \quad (4.5)$$

$$w = t + \frac{x}{c} + \frac{a}{c} \ln|1 - \exp(-2x/a)| , \quad (4.6)$$

and the acoustic spacetime is represented in figure 4. The acoustic horizon is again at  $x = 0$  and the surface gravity is again  $\kappa = c/a$ .

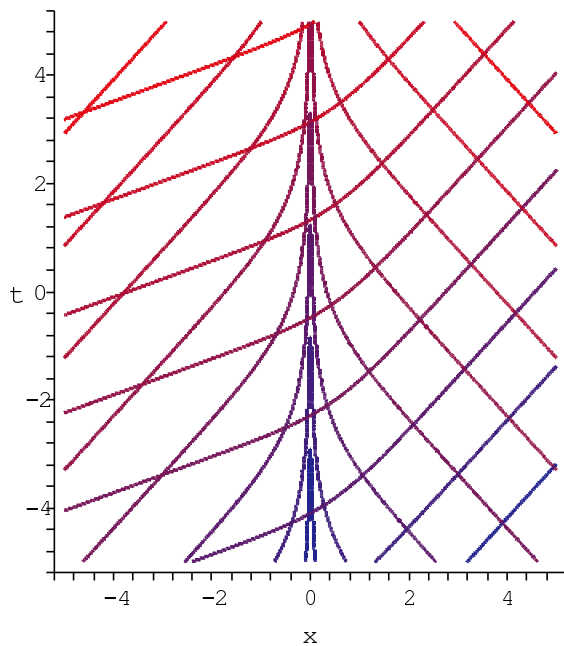


Figure 4: Acoustic white hole.  $u = \text{const}$  are the blue lines,  $w = \text{const}$  are the red lines.

### 4.1.3 Black hole, non-physical

Consider a left-going flow, one subsonic region, one supersonic; but with the flow velocity  $v$  now unbounded. For example, take

$$v(x) = -c \exp(-x/a) \quad (4.7)$$

(as sketched in figure 5), which leads to

$$u = t - \frac{x}{c} - \frac{a}{c} \ln |1 - \exp(-x/a)|, \quad (4.8)$$

$$w = t + \frac{x}{c} + \frac{a}{c} \ln(1 + \exp(-x/a)), \quad (4.9)$$

and to the acoustic spacetime of figure 6. From a laboratory point of view, this configuration is unphysical, as the velocity of the flow grows without limit. Though unphysical when interpreted in terms of a flowing fluid, we have nevertheless included this example here because it is similar to what actually happens in a Schwarzschild black hole when it is put into “acoustic form”. In Painlevé-Gullstrand coordinates the velocity profile associated with a Schwarzschild black hole ( $v_S \propto 1/\sqrt{r}$ ; see [5] for example) grows without limit once the horizon is crossed. The divergence of the velocity profile there signals the appearance of a singularity. Here, the same happens as  $x \rightarrow -\infty$ . Indeed, the Ricci scalar (which, in two dimensions, contains all the information about curvature) for the acoustic metric (2.10) is, when  $v$  does not depend on  $t$ ,

$$R = \frac{1}{c^2 \Omega^2} \frac{d^2 v^2}{dx^2} + \text{terms containing derivatives of } \Omega. \quad (4.10)$$

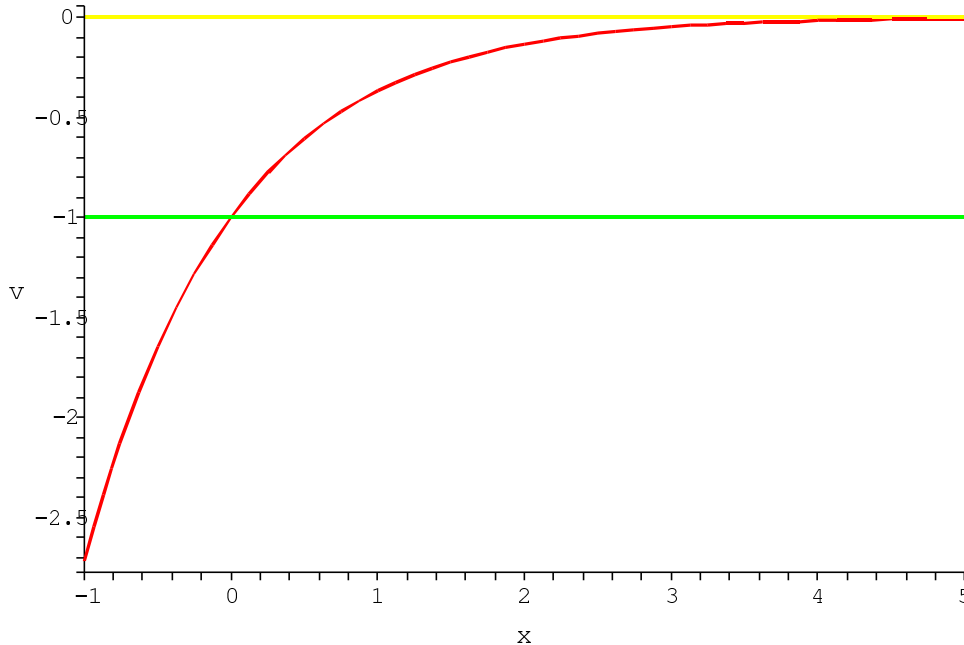


Figure 5: Velocity profile for an unphysical black hole. There is again a left-going flow, one subsonic region, one supersonic, but now  $v$  is unbounded.

For the velocity profile (4.7) this becomes

$$R = \frac{4}{a^2 \Omega^2} \exp(-2x/a) + \text{terms containing derivatives of } \Omega, \quad (4.11)$$

which, for a regular  $\Omega$ , diverges when  $x \rightarrow -\infty$ , indicating the presence of a curvature singularity. Indeed, all of the standard curvature invariants diverge exponentially as  $x \rightarrow -\infty$ .

The difference with respect to the Schwarzschild black hole is that there, the divergence appears at a finite coordinate distance. However, in both cases the proper distance<sup>3</sup> from a point beyond the horizon to the singularity is finite. We will discuss this point further in section 8. For the specific example given above, the horizon is again at  $x = 0$  and the surface gravity is again  $\kappa = c/a$ .

#### 4.1.4 Extremal black hole

Consider now a left-going flow, with one sonic point, and no supersonic region:

$$v(x) = -\frac{c}{\cosh(x/a)} \quad (4.12)$$

(figure 7). For obvious reasons, we call this acoustic geometry extremal because the derivative of the velocity profile with respect to  $x$  vanishes at  $x_S$ . Equivalently, the parameter

<sup>3</sup>In fact, proper time, as the coordinate  $r$  (or  $x$  in this particular case) changes its spatial character to a timelike character beyond the horizon.

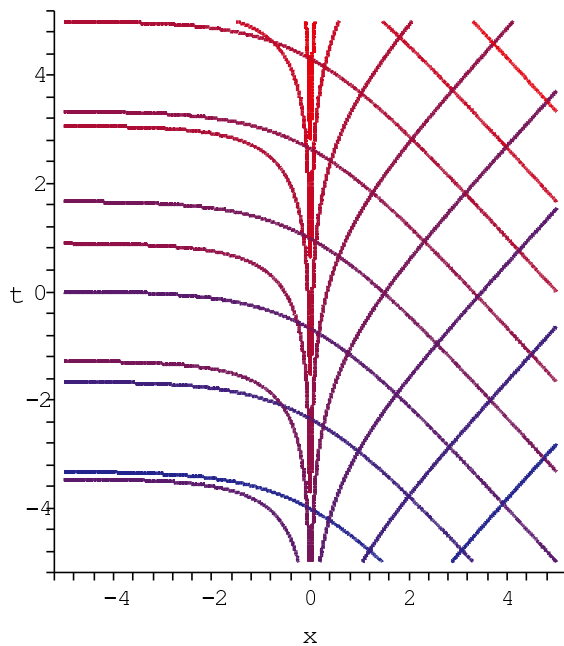


Figure 6: Unphysical acoustic black hole.  $u = \text{const}$  are the blue lines,  $w = \text{const}$  are the red lines.

$\kappa$ , representing the surface gravity at the horizon, vanishes. This is exactly what happens in a Reissner–Nordström extremal geometry. The velocity profile (in Painlevé–Gullstrand coordinates) for a Reissner–Nordström extremal black hole is

$$v(r)^2 = -\frac{2M}{r} + \frac{M^2}{r^2}. \quad (4.13)$$

Once the horizon at  $r_H = M$  is crossed, the velocity starts to decrease until it becomes zero at  $r = M/2$ . The quantity  $v(r)^2$  then changes sign and grows without limit, forming a singularity at  $r = 0$ . In a condensed matter laboratory this profile would be unphysical, in particular since the velocity would be imaginary, so the closest we can get is to make the velocity profile decrease progressively towards zero once the horizon is crossed. (Modifications of the Painlevé–Gullstrand coordinates for the Reissner–Nordström geometry that avoid these imaginary velocities have been discussed by Volovik [18], see also [19].)

The null coordinates for this example are

$$u = t - \frac{x}{c} + \frac{2a}{c(\exp(x/a) - 1)}; \quad (4.14)$$

$$w = t + \frac{x}{c} + \frac{2a}{c(\exp(x/a) + 1)}. \quad (4.15)$$

The acoustic spacetime is represented in figure 8. The horizon occurs at  $x = 0$  and by construction  $\kappa = 0$ .

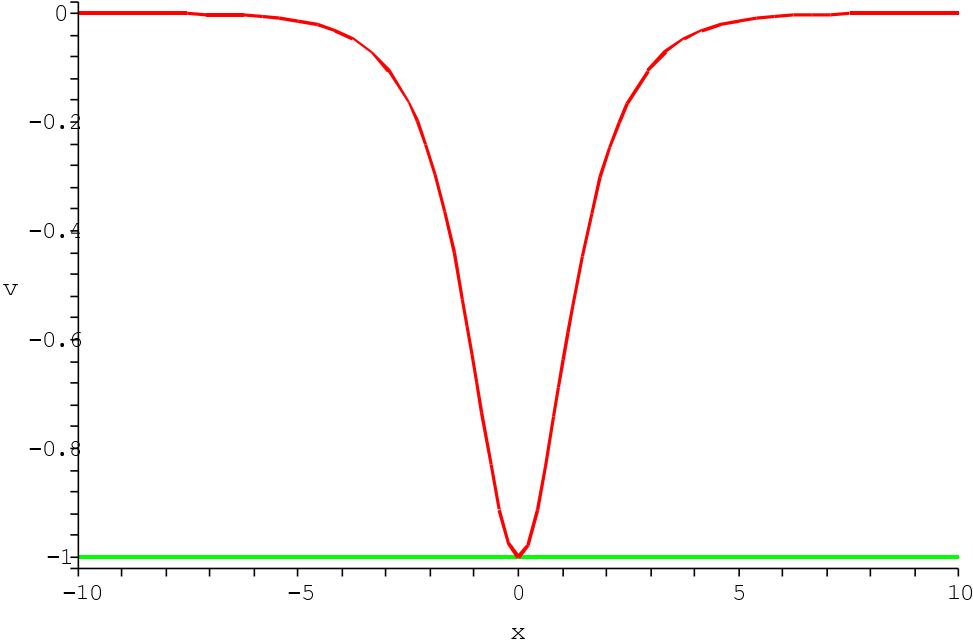


Figure 7: Extremal black hole. Velocity profile for a left-going flow, one sonic point, no supersonic region.

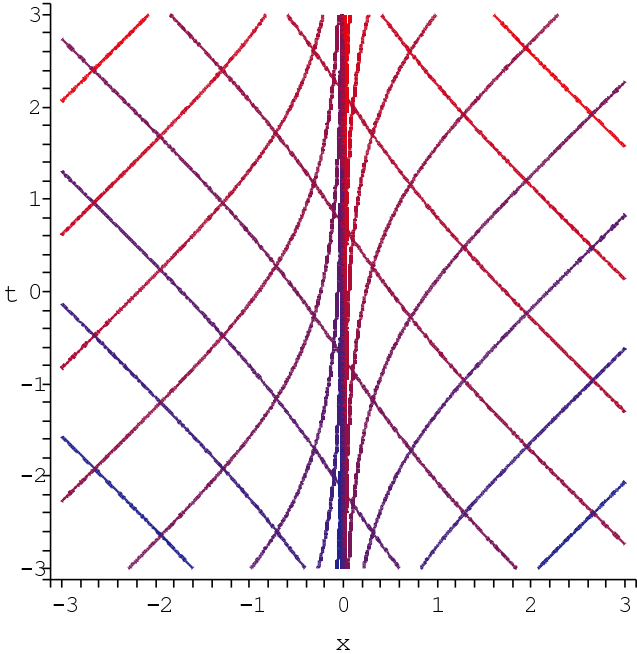


Figure 8: Extremal black hole.  $u = \text{const}$  are the blue lines,  $w = \text{const}$  are the red lines. This is qualitatively indistinguishable from a critical black hole spacetime.

#### 4.1.5 Critical black hole

Consider now a left-going flow, with one sonic point, no supersonic region, but with a singular flow at the horizon. For example

$$v(x) = -\frac{2c}{\exp(2|x|/a) + 1} \quad (4.16)$$

(figure 9). The major difference is now that, because of the dependence on the absolute value of  $x$ , the velocity profile changes abruptly at the sonic point. The null coordinates

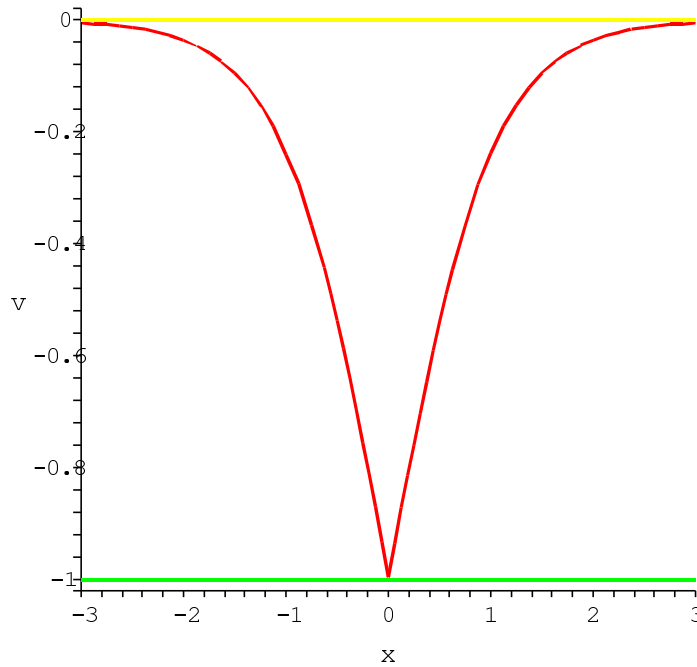


Figure 9: Critical black hole: Velocity profile for a left-going flow, one sonic point, no supersonic region, but singular flow at the sonic point.

for this example are:

$$u = \begin{cases} t - \frac{x}{c} - \frac{a}{c} \ln \left( \frac{\exp(-2x/a)}{\exp(-2x/a) - 1} \right) & \text{for } x < 0; \\ t - \frac{x}{c} + \frac{a}{c} \ln \left( \frac{\exp(2x/a)}{\exp(2x/a) - 1} \right) & \text{for } x > 0; \end{cases} \quad (4.17)$$

$$w = \begin{cases} t + \frac{x}{c} - \frac{a}{3c} \ln \left( \frac{4 \exp(-2x/a)}{\exp(-2x/a) + 3} \right) & \text{for } x < 0; \\ t + \frac{x}{c} + \frac{a}{3c} \ln \left( \frac{4 \exp(2x/a)}{\exp(2x/a) + 3} \right) & \text{for } x > 0. \end{cases} \quad (4.18)$$

This acoustic geometry is similar to that of the extremal case (see figure 8) in that at the sonic point the velocity of the flow does not change from subsonic to supersonic, but

comes back to subsonic. The important difference is that at the horizon the one-sided surface gravity  $\kappa$  is now different from zero.

Indeed the horizon is located at  $x = 0$ , and if the surface gravity is calculated in a one-sided manner from either side of the horizon we find  $\kappa = c/a$ . However if the surface gravity is evaluated by taking a two-sided symmetric limit then  $\kappa = 0$ . This is a result of the abrupt change in velocity profile at the horizon, so that this particular model spacetime exhibits some features of both extremal and non-extremal geometries. This aspect of the model is particularly interesting and might be important when analyzing the Hawking process of quantum emission from the vacuum (we leave this analysis for a follow-up paper).

## 4.2 Flows with two sonic points

Let us now consider the description of stationary but otherwise arbitrary (1+1)-dimensional acoustic geometries in which there are two sonic points.

### 4.2.1 Black and white hole combination

Such a combination can be realised by a left-going flow, with two subsonic regions, and one supersonic region located between them. Consider for example

$$v(x) = -\frac{c\alpha}{\cosh(x/a)}, \quad (4.19)$$

with  $\alpha > 1$  (figure 10). The two sonic points are  $x_S = x_1$  and  $x_S = x_2$ , with

$$x_{1,2} = a \ln(\alpha \mp \sqrt{\alpha^2 - 1}). \quad (4.20)$$

The null coordinates for this example are:

$$u = t - \frac{x}{c} - \frac{\alpha a}{c\sqrt{\alpha^2 - 1}} \ln \left| \frac{1 - (\alpha + \sqrt{\alpha^2 - 1}) \exp(-x/a)}{1 - (\alpha - \sqrt{\alpha^2 - 1}) \exp(-x/a)} \right|; \quad (4.21)$$

$$w = t + \frac{x}{c} + \frac{\alpha a}{c\sqrt{\alpha^2 - 1}} \ln \left| \frac{1 + (\alpha + \sqrt{\alpha^2 - 1}) \exp(-x/a)}{1 + (\alpha - \sqrt{\alpha^2 - 1}) \exp(-x/a)} \right|. \quad (4.22)$$

The acoustic spacetime is shown in figure 11. Of course, from the point of view of observers located in the asymptotic region on the right ( $x \rightarrow +\infty$ ) there is just a black hole. However, observers lying in the middle region with  $x_1 < x < x_2$  will experience both a future and a past event horizon, with the corresponding black and white hole regions.

This is the non-extremal version of the configuration considered in section 4.1.4, which corresponds to the choice  $\alpha = 1$ . The surface gravity

$$\kappa = \frac{c}{a} \frac{\sqrt{\alpha^2 - 1}}{\alpha} \quad (4.23)$$

is now different from zero. This class of acoustic geometries, and the ring geometry to be considered below, is of particular interest for any realistic attempt at building acoustic analogue black holes in the laboratory.



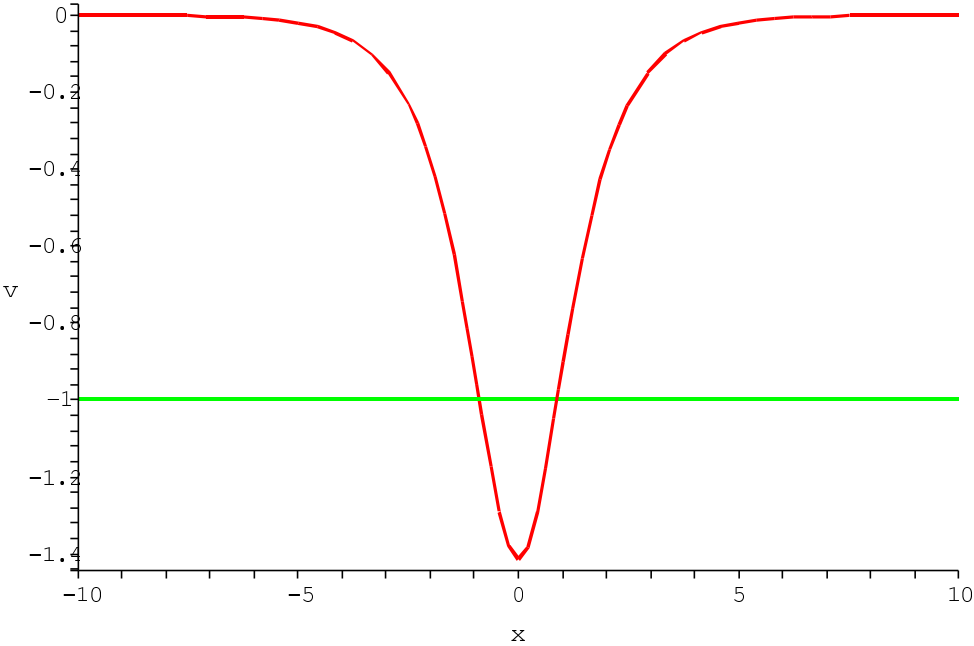


Figure 10: Velocity profile for a black hole–white hole combination: A left-going flow, two subsonic regions, one supersonic region sandwiched between them;  $\alpha = \sqrt{2}$ .

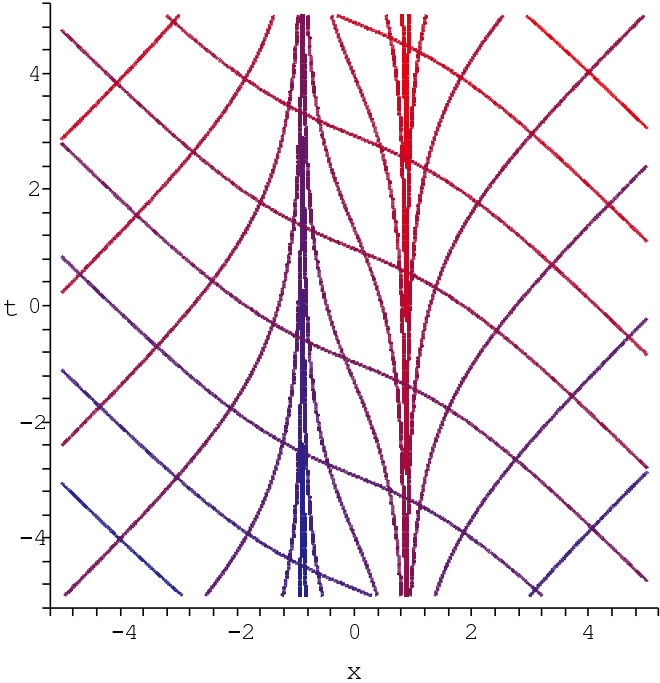


Figure 11: Black hole–white hole configuration.  $u = \text{const}$  are the blue lines,  $w = \text{const}$  are the red lines;  $\alpha = \sqrt{2}$ .

### 4.2.2 Ring configuration

Consider a left-going flow in a ring. Assume one supersonic region, one subsonic, and  $v$  bounded. For example, we could take

$$v(x) = -\frac{\alpha c}{2} \left( 1 + \cos \frac{\pi x}{L} \right) \quad (4.24)$$

with  $\alpha > 1$  (otherwise there are no sonic points) and  $L$  equal to half of the ring length (the ring goes from  $-L$  to  $L$ ); see figure 12. This configuration, because the working fluid is constantly recycled, is perhaps the premier class of acoustic models that are potentially of experimental interest [6, 20, 21, 22].

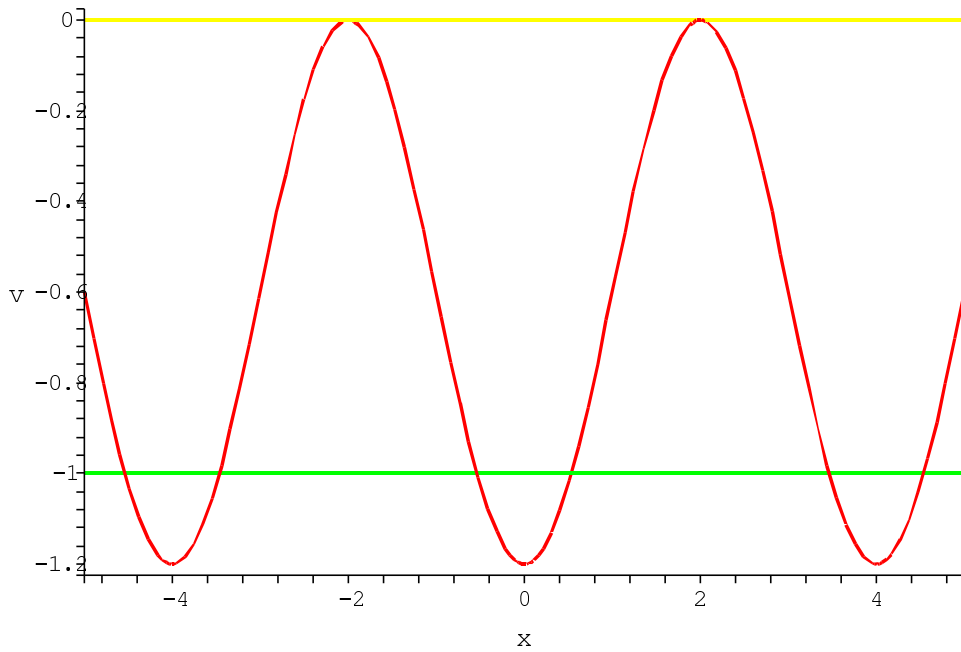


Figure 12: Ring configuration: Velocity profile for a left-going flow, in a ring with one supersonic region;  $\alpha = 1.2$ ;  $L = 2$ .

The null coordinates are

$$u = t + \frac{L}{c\pi\sqrt{\alpha-1}} \ln \left| \frac{\sqrt{\alpha-1} + \tan \frac{\pi x}{2L}}{\sqrt{\alpha-1} - \tan \frac{\pi x}{2L}} \right|, \quad (4.25)$$

$$w = t + \frac{2L}{c\pi\sqrt{\alpha+1}} \arctan \left( \frac{1}{\sqrt{\alpha+1}} \tan \frac{\pi x}{2L} \right), \quad (4.26)$$

and the acoustic spacetime is shown in figure 13. The black (+) and white (-) hole horizons occur at

$$x_S = \pm \frac{L}{\pi} \arccos \left( \frac{2}{\alpha} - 1 \right) \quad (4.27)$$

with surface gravity

$$\kappa = \frac{c\pi\sqrt{\alpha-1}}{L}. \quad (4.28)$$

We note that because of the periodicity in space it is not possible to define absolute horizons (event horizons) in the normal way. Whenever we speak of horizons in the ring configuration we will be referring primarily to apparent horizons which we can define in a local manner. If the apparent horizon asymptotes to a null curve in the infinite future (or infinite past) then a null curve that is tangent to this asymptote is the best global definition of a horizon that one could hope to achieve.

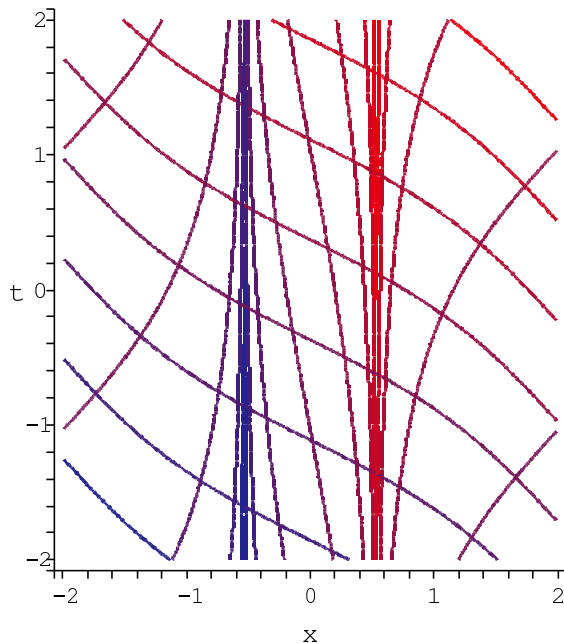


Figure 13: Ring-hole: Black hole–white hole configuration with periodic boundary conditions.  $u = \text{const}$  are the blue lines,  $w = \text{const}$  are the red lines.  $\alpha = 1.2$ ;  $L = 2$ . While the technical definition of the absolute horizon does not work in this situation, the apparent horizons are located symmetrically about the origin.

### 4.2.3 Two black holes

As a final example in our collection of stationary examples we consider a system containing two supersonic regions, with one subsonic region trapped between them,  $v$  remaining bounded. A simple example of this configuration is given by the velocity profile

$$v(x) = -c\alpha \tanh(x/a) , \quad (4.29)$$

with  $\alpha > 1$ ; see figure 14. (To build such a flow in a condensed matter system one would clearly need to somehow remove fluid from the vicinity of the origin in order to be compatible with the equation of continuity. An example of such behaviour occurs in certain Bose-Einstein condensate-inspired models of analog black holes where an outcoupling laser beam focused on the origin is used to systematically destroy the condensate and set up opposing supersonic flows into the origin [6, 20, 21].) The null coordinates are

$$u = t + \frac{x}{c(\alpha - 1)} + \frac{\alpha a}{c(\alpha^2 - 1)} \ln \left| 1 - \frac{\alpha + 1}{\alpha - 1} \exp(-2x/a) \right| , \quad (4.30)$$

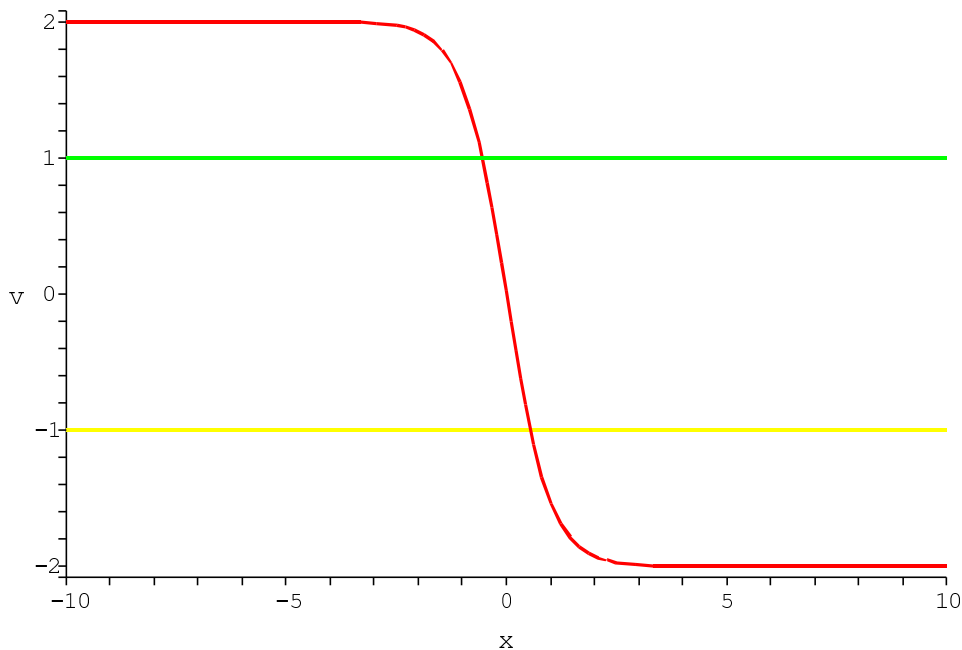


Figure 14: Two black hole configuration: Velocity profile for a left-going flow, two supersonic regions, one subsonic trapped between them;  $v$  bounded;  $\alpha = 2$ .

$$w = t + \frac{x}{c(\alpha + 1)} + \frac{\alpha a}{c(\alpha^2 - 1)} \ln \left| 1 - \frac{\alpha - 1}{\alpha + 1} \exp(-2x/a) \right| , \quad (4.31)$$

and the spacetime is represented in figure 15. The horizons are located at

$$x_S = \pm a \ln \left( \frac{\alpha + 1}{\alpha - 1} \right) \quad (4.32)$$

and the surface gravity is

$$\kappa = \frac{c}{a} \left( \alpha - \frac{1}{\alpha} \right) . \quad (4.33)$$

This completes our exhibition of stationary configurations. Additional examples can be constructed via parity reflection or time reversal but there are no significant new insights to be gained from such an exercise. We shall now turn to the question of classifying time-dependent acoustic geometries and begin by making some general comments.

## 5 Dynamical zoo

Let  $\sigma(t)$  be some smooth function that increases monotonically from 0 (for  $t \rightarrow -\infty$ ) to 1 (for  $t \rightarrow +\infty$ ); for example,

$$\sigma(t) = \frac{1}{2} [1 + \tanh(t/t_0)] , \quad (5.1)$$

where  $t_0$  is a positive constant. Then, for any  $\bar{v}(x)$ , the function  $v(t, x) := \sigma(t) \bar{v}(x)$  represents a velocity profile that changes in time from 0 to  $\bar{v}(x)$ . In particular, we can choose for  $\bar{v}(x)$  any one of the functions considered in the previous examples.

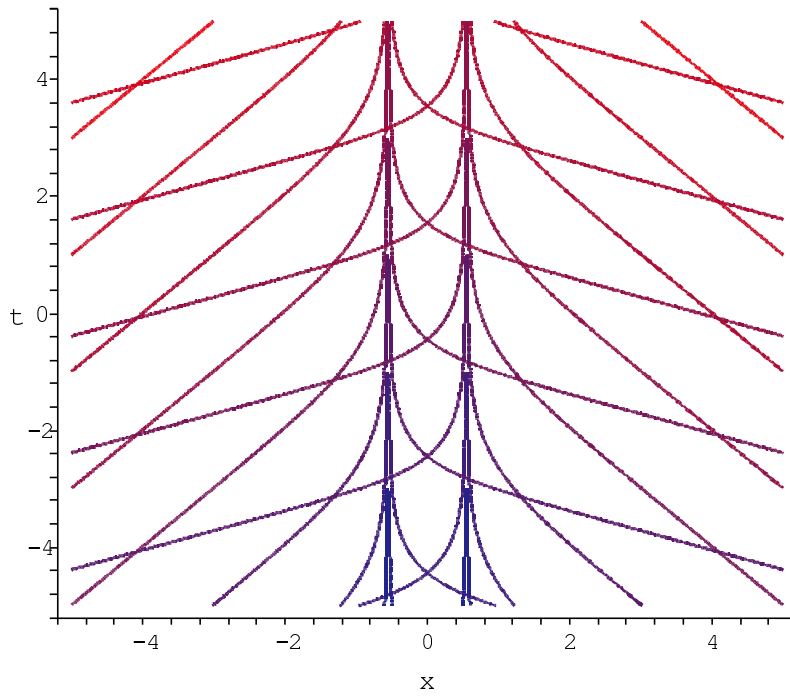


Figure 15: Two black hole configuration.  $u = \text{const}$  are the blue lines,  $w = \text{const}$  are the red lines;  $\alpha = 2$ .

The differential equations for the worldlines of right-going and left-going sound rays are, respectively:

$$\left(\frac{dt}{dx}\right)_R = \frac{1}{c + v(t, x)}; \quad (5.2)$$

$$\left(\frac{dt}{dx}\right)_L = -\frac{1}{c - v(t, x)}. \quad (5.3)$$

Integrating these equations is not an easy task, even for very specific and simple choices of the functions  $\sigma$  and  $\bar{v}$ . However, we can readily identify the apparent acoustic horizons, where

$$\sigma(t) \bar{v}(x) = \pm c. \quad (5.4)$$

At the apparent horizons, either  $(dt/dx)_R$  or  $(dt/dx)_L$  becomes infinite, that is, the signal world lines (the  $u = \text{const}$  and  $w = \text{const}$  curves) have a vertical tangent in the  $(t, x)$  diagram. Other features of relevance are that when  $t \rightarrow -\infty$ , where we have both  $(dt/dx)_R \rightarrow 1/c$  and  $(dt/dx)_L \rightarrow -1/c$ , the acoustic spacetime becomes Minkowskian. In contrast, for  $t \rightarrow +\infty$ , where

$$\left(\frac{dt}{dx}\right)_R \sim \frac{1}{c + \bar{v}(x)}, \quad (5.5)$$

$$\left(\frac{dt}{dx}\right)_L \sim -\frac{1}{c - \bar{v}(x)}, \quad (5.6)$$

we see that the structure of spacetime resembles those previously considered in the stationary cases. Therefore this class of acoustic geometries can be viewed as providing simple and concrete examples of black hole and white hole formation in situations where the underlying physics is very simple and completely under control. Let us now pass to more specific descriptions of the behaviour of these dynamical acoustic geometries.

## 5.1 Flows developing one sonic point

### 5.1.1 Black hole

Figure 16 represents the effect of switching on a single horizon black hole. As such it is a simple model for what would in standard general relativity correspond to a collapse process, and one can easily formulate and analyze questions regarding the apparent and absolute horizons and easily verify that they are markedly different. An interesting feature is the fact that the absolute horizon (the event horizon) extends all the way back to  $t = -\infty$  in a region where the acoustic geometry is approximately flat (Minkowskian). This is a concrete physical example of the fact that the absolute horizon, unlike the apparent horizon, is “teleological” [23, 24, 25, 26]. It is easy to fall into the trap of thinking that the absolute horizon “knows” that supersonic flow will be established sometime in the future. Instead what is happening is more subtle — the technical definition of the absolute horizon requires complete information of the entire future history of the spacetime, and so the fact that the absolute horizon extends into regions where there is no fluid flow is merely a retrodiction, from the point of view of the infinite future, as to which regions of the spacetime could have communicated with which parts of future null infinity. The absolute horizon is not akin to a physical membrane, and is completely undetectable by any local experiment. The apparent horizon, in contrast, can be formulated and detected in terms of local physics.

Such behaviour also occurs in standard general relativity, where it is a reasonably easy exercise to construct spacetimes with event horizons that first form in regions of the spacetime that are Riemann-flat, and hence completely curvature-free.

### 5.1.2 White hole

Similarly, figure 17 represents the effect of switching on a single white hole horizon. Note that the location of the apparent horizon is the same as in the black hole case, while the location of the event horizon is mirror reversed.

### 5.1.3 Black hole, non-physical

The situation in figure 18 is “unphysical” in the sense that the fluid velocity goes to infinity at one spatial limit. Though this is bad from the point of view of a real physical fluid flow, it is actually rather close to the situation that arises in a collapse to a Schwarzschild black hole, wherein the Painlevé–Gullstrand “velocity” does tend to infinity at the central singularity.

### 5.1.4 Extremal black hole

In figure 19 we see the phenomenon of switching on an extremal black hole. The apparent horizon is now simply an isolated point in the infinite future, while the location of the

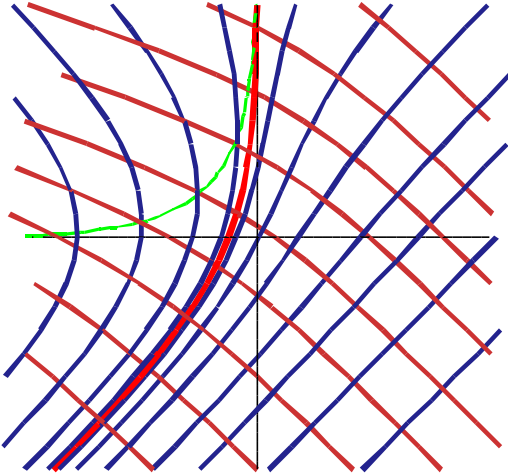


Figure 16: Switching on an acoustic black hole.  $u = \text{const}$  are the blue lines,  $w = \text{const}$  are the red lines. The green line is the apparent horizon. The thick red line is the event horizon.

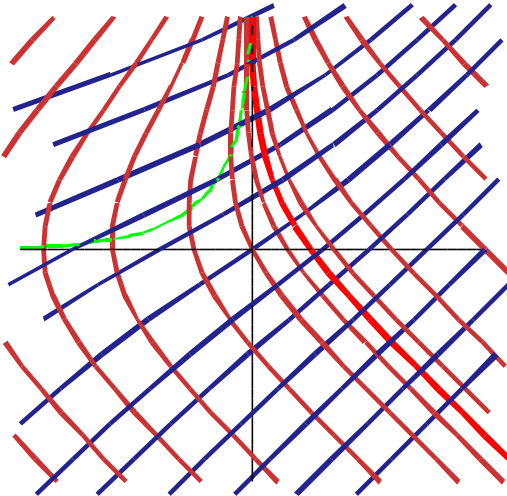


Figure 17: Formation of an acoustic white hole.  $u = \text{const}$  are the blue lines,  $w = \text{const}$  are the red lines. The green line is the apparent horizon. The thick red line is the event horizon.

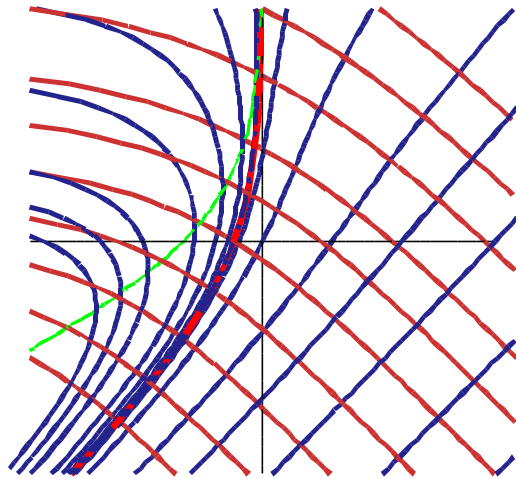


Figure 18: Switching on an unphysical acoustic black hole.  $u = \text{const}$  are the blue lines,  $w = \text{const}$  are the red lines. The green line is the apparent horizon. The thick red line is the event horizon.

event horizon asymptotes to its known position in the stationary case.

### 5.1.5 Critical black hole

Switching on a critical black hole, is qualitatively similar to switching on an extremal black hole, hence see again figure 19 above. An interesting point is that in order for the horizon to form the interpolating function  $\sigma(t)$  must approach unity with sufficient rapidity. In particular the existence or not of an event horizon on these geometries will depend on the possibility of sending signals from the left-hand-side that then reach the right-hand-side infinity.

In order to see this let us start by noticing that the velocity of such right-moving signals is given by equation (5.2) and takes the form

$$\frac{dx}{dt} = c - v(x, t) = c - \sigma(t)\bar{v}(x). \quad (5.7)$$

where here  $\bar{v}$  is the absolute value of the velocity. At very late times  $t \rightarrow +\infty$  we can write  $\sigma(t) = 1 - A(t)$  where now  $A(t)$  encodes the way  $\sigma(t)$  approaches unity. We can then write

$$\frac{dx}{dt} = c - v(x, t) = A(t)\bar{v}(x) + c - \bar{v}(x), \quad (5.8)$$

but we know that  $c - \bar{v}(x) \geq 0$  at all times so that

$$\frac{dx}{dt} \geq A(t)\bar{v}(x). \quad (5.9)$$



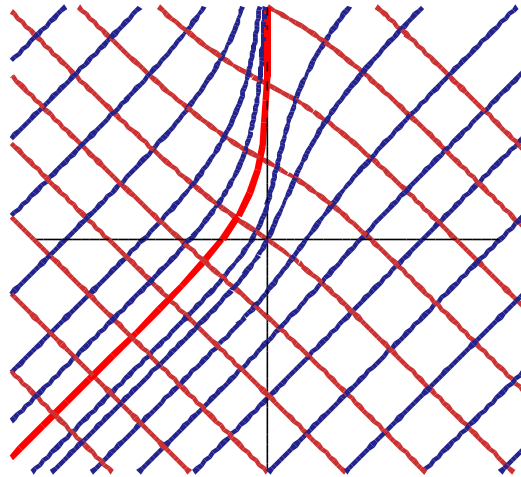


Figure 19: Switching on an extremal black hole.  $u = \text{const}$  are the blue lines,  $w = \text{const}$  are the red lines. The apparent horizon is a single isolated point. The thick red line is the event horizon. This diagram is qualitatively indistinguishable from that describing the formation of a critical black hole.

Integrating this inequality we have

$$\int_{x_i}^{x_\infty} \frac{dx}{\bar{v}(x)} \geq \int_{t_i}^{+\infty} A(t) dt, \quad (5.10)$$

where  $x_\infty$  is the location of the right-moving sound ray at time  $t = +\infty$ . Now the convergence or otherwise of the right-hand-side integral depends on the specific form of  $A(t)$ . For example, for  $A(t) = Ne^{-t/t_0}$  [which is the late-time behaviour we deduce from the  $\sigma(t)$  we chose in (5.1)] or for another example taking  $A(t) = N/t^n$ , with  $n > 1$ , we have that this left-hand-side integral yields a finite result. The inequality then permits  $x_\infty$  to be finite, and therefore we deduce that in these situations there can be right-moving signals not able to reach the asymptotic right infinity: An event horizon can be formed (though it is not guaranteed to be formed by the current argument). In contrast, for  $A(t) = Nt^{-n}$ , with  $0 < n \leq 1$ , this integral diverges and thus from the inequality we deduce  $x_\infty \rightarrow +\infty$ . So no event horizon can possibly be formed in the dynamical process. Again, this might have important implications when analyzing the Hawking process on these backgrounds.

## 5.2 Flows developing two sonic points

When we turn to dynamical situations with two sonic horizons we again note that the behaviour of apparent and absolute horizons can differ markedly from each other.

### 5.2.1 Black and white hole

When switching on a black hole–white hole combination, as in figure 20, note that the apparent horizon loops back from one absolute horizon to the other, asymptoting to both absolute horizons in the far future.

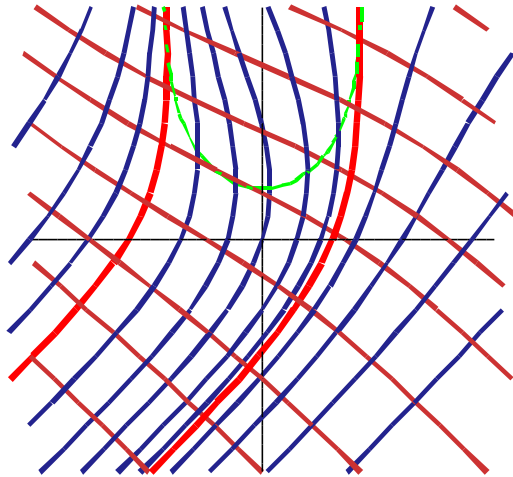


Figure 20: Formation of a black hole–white hole configuration.  $u = \text{const}$  are the blue lines,  $w = \text{const}$  are the red lines. The green line is the apparent horizon. The two thick red lines are the event horizons.  $\alpha = \sqrt{2}$ .

### 5.2.2 Ring configuration

In figures 21 and 22 we see the effect of switching on supersonic flow in a ring geometry. The first figure emphasises the structure of the fundamental region, whereas the second diagram emphasises the periodic nature of the ring geometry.

### 5.2.3 Two black holes

Note that in figure 23, where a pair of black holes is switched on by effectively sucking fluid into the origin [6, 20, 21], the geometry is reflection invariant.

## 6 Compactification — Stationary geometries

We now present the Penrose–Carter conformal diagrams [24, 25, 27, 28] for the various cases in the previous zoos. These diagrams are used to exhibit the global causal structure of the model spacetimes we are considering. The basic idea underneath the conformal diagram of any non-compact 1+1 manifold is that its metric can always be conformally mapped to the metric of a compact geometry, with a boundary added to represent events

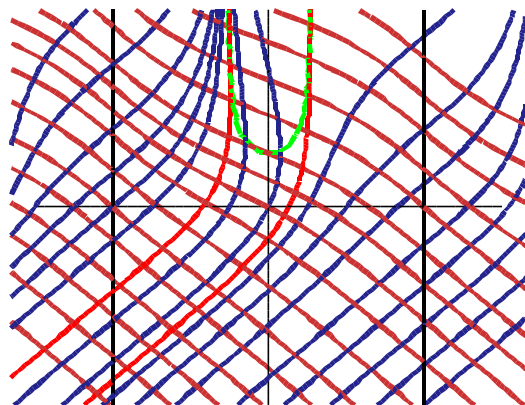


Figure 21: Formation of a supersonic region in a ring flow.  $u = \text{const}$  are the blue lines,  $w = \text{const}$  are the red lines. The apparent horizon is the green line. The two thick red lines are the “event horizons”, defined as null curves that are tangent to the asymptotic future limit of the apparent horizons.  $\alpha = 1.2$ ;  $L = 2$ .

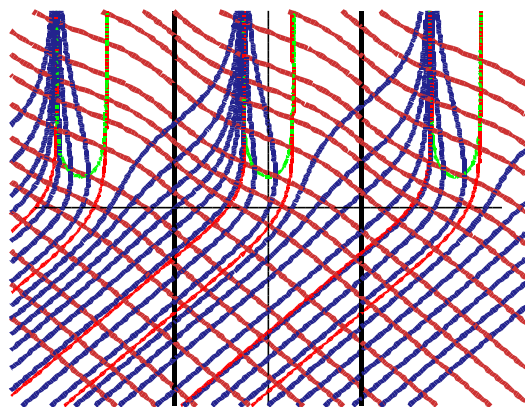


Figure 22: Formation of a supersonic region in a ring flow with periodicity exposed.  $u = \text{const}$  are the blue lines,  $w = \text{const}$  are the red lines. The apparent horizon is the green line. The thick red lines are the event horizons. Here, the “event horizons” are defined as null curves that are tangent to the asymptotic future limit of the apparent horizons.  $\alpha = 1.2$ ;  $L = 2$ .

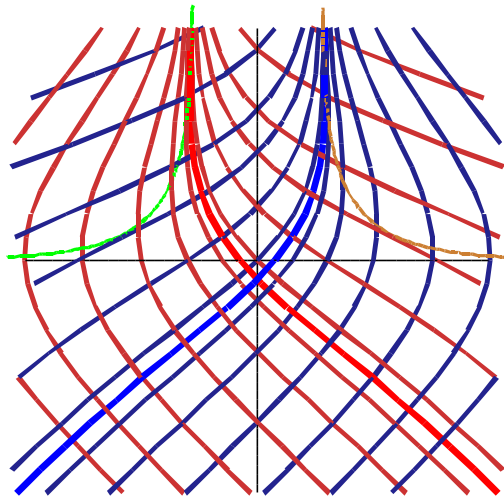


Figure 23: Formation of a two black hole configuration.  $u = \text{const}$  are the blue lines,  $w = \text{const}$  are the red lines. The green and gold lines are the apparent horizons. The thick red line and thick blue line are the two event horizons, which cross at a finite time.  $\alpha = 2$ .

at infinity. Since compact spacetimes are in some sense “finite”, they can then properly be drawn on a sheet of paper.

To accomplish this, one way is to use coordinates that are regular across the horizons and that reach finite values at infinity. The null coordinates  $u$  and  $w$  are clearly unsuitable, since they diverge when  $v = -c$  or  $v = c$ , respectively, as seen in section 3. However, we can introduce new coordinates in the same way in which one defines Kruskal coordinates for Schwarzschild spacetime [24, 25, 28]. Let  $U(u)$  and  $W(w)$  be new null coordinates. The metric (3.3) with  $F = G = 1$  becomes

$$g = -\Omega^2 (c^2 - v^2) \frac{du}{dU} \frac{dw}{dW} dU dW , \quad (6.1)$$

where everything is expressed in terms of  $U$  and  $W$  as independent variables. Then, the strategy is to choose the functions  $U(u)$  and  $W(w)$  in such a way that the coefficient

$$\Omega^2 (c^2 - v^2) \frac{du}{dU} \frac{dw}{dW} \quad (6.2)$$

be regular everywhere.

For example, consider a flow which has a single sonic point with  $v = -c$  at  $x = 0$ , like the one of section 4.1.1. From equations (3.6) we find

$$w - u \sim \frac{x}{2c} + \frac{1}{\kappa} \ln |x| . \quad (6.3)$$

As we approach  $x = 0$  the coordinate  $u$  grows indefinitely, while  $w$  remains finite. Therefore  $w - u \sim -u$  and equation (6.3) can be simplified near the sonic point as

$$|x| \sim \exp(-\kappa u) . \quad (6.4)$$

Then, near  $x = 0$  we have

$$c^2 - v^2 \sim 2 \epsilon c \kappa x \sim 2 \epsilon c \kappa \frac{x}{|x|} \exp(-\kappa u) , \quad (6.5)$$

where equation (3.4) has been used in the first step. Hence, in order to keep the coefficient (6.2) finite, it is sufficient that  $dU/du$  be proportional to the expression on the right-hand side of equation (6.5). Thus we choose, near the sonic point  $x = 0$ ,

$$U(u) \propto -\frac{x}{|x|} \exp(-\kappa u) , \quad (6.6)$$

with a positive proportionality factor, so that  $U$  varies regularly from  $-\infty$  to  $+\infty$  as  $x$  varies from  $+\infty$  to  $-\infty$ . On the other hand,  $w$  is regular everywhere, so we can choose for  $W$  any regular monotonic function of  $w$  such that  $W(\pm\infty) = \pm\infty$ .

Let us now choose the new coordinates

$$\mathcal{U} := \arctan U, \quad \mathcal{W} := \arctan W, \quad (6.7)$$

that take values in the range  $(-\pi/2, \pi/2)$ . The acoustic metric is

$$g = -\Omega^2 \frac{c^2 - v^2}{\cos^2 \mathcal{U} \cos^2 \mathcal{W}} \frac{du}{dU} \frac{dw}{dW} d\mathcal{U} d\mathcal{W} , \quad (6.8)$$

where everything is expressed as a function of  $\mathcal{U}$  and  $\mathcal{W}$ . Hence, the metric is conformal to

$$\bar{g} = -d\mathcal{U} d\mathcal{W} , \quad (6.9)$$

so the causal structure of the spacetime is identical to the one of the portion  $(\mathcal{U}, \mathcal{W}) \in (-\pi/2, \pi/2) \times (-\pi/2, \pi/2)$  of Minkowski spacetime. The points on the boundary, where  $\mathcal{U}$  and  $\mathcal{W}$  attain values  $\pm\pi/2$ , represent sonic boundaries or points at infinity in the acoustic spacetime. We now consider the Penrose–Carter conformal diagrams for the various acoustic geometries we have investigated.

## 6.1 Flows with one sonic point

### 6.1.1 Black hole

For the case of a single isolated black hole horizon we find the Penrose–Carter diagram of figure 24.<sup>4</sup> As we have already commented, in the acoustic spacetimes with no periodic identifications there are two clearly differentiated notions of asymptotia, “right” and “left”. In all our figures we have used subscripts “right” and “left” to label the different null and spacelike infinities. In addition, we have denoted the different sonic-point boundaries with  $\mathfrak{S}_{\text{right}}^{\pm}$  or  $\mathfrak{S}_{\text{left}}^{\pm}$  depending on whether they are the starting point (− sign) or the ending point (+ sign) of the null geodesics in the right or left parts of the diagram.

In contradistinction to the Penrose–Carter diagram for the Schwarzschild black hole (which in the current context would have to be an eternal black hole, not one formed via astrophysical stellar collapse) there is no singularity. On reflection, this feature of the conformal diagram should be obvious since the fluid flow underlying the acoustic geometry is nowhere singular. Note that the event horizon  $\mathcal{H}$  is the boundary of the causal past of future right null infinity; that is,  $\mathcal{H} = \dot{J}^-(\mathfrak{S}_{\text{right}}^+)$ , with standard notations [24, 25, 28].

<sup>4</sup>In the figure we have introduced an aspect ratio different from unity for the coordinates  $\mathcal{U}$  and  $\mathcal{W}$ , in order to make the various regions of interest graphically more clear.

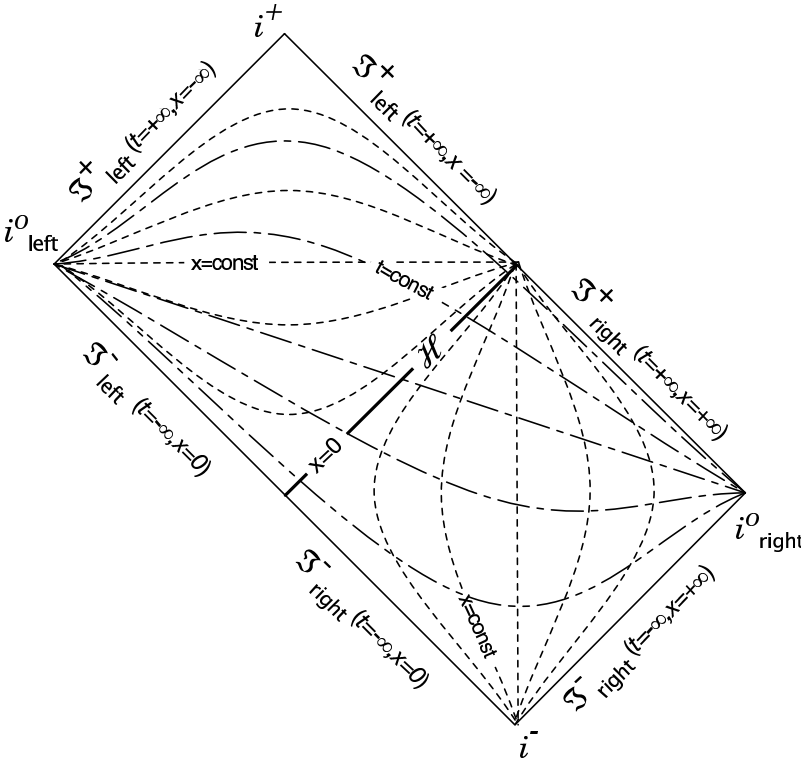


Figure 24: Conformal diagram of an acoustic black hole.

### 6.1.2 White hole

The Penrose–Carter diagram for a single white hole horizon, as presented in figure 25, does not provide any new surprises. Again note the absence of any singularity. Though this is a simple observation we feel it should be emphasised: These last two very simple examples conclusively demonstrate that the existence of black hole and white hole absolute horizons (event horizons) does not require the presence of any geometrical singularity anywhere in the spacetime. That event horizons in general relativity are always related to the presence of some sort of curvature singularity is a geometrodynamical statement that depends specifically on the use of the vacuum Einstein equations, or on the use of specific matter models plus the Einstein equations [25]. Since the geometry of acoustic spacetimes is not governed by the Einstein equations, we can very easily come up with global causal structures that are more general than those encountered within the context of standard general relativity. The utility of doing so is twofold:

- If one wishes to physically build an acoustic spacetime, say with a view to experimentally probing curved-space quantum field theory [1, 6, 22, 29, 30, 31, 32, 33, 34], it is very useful to know how these spacetimes can differ from those in standard general relativity.
- If in contrast one is interested in studying extensions to standard general relativity, then these particularly simple acoustic spacetimes provide concrete examples that can be used as a guide to the types of generalization that are in principle possible.

Note that in this situation the event horizon  $\mathcal{H}$  is the boundary of the causal future of past right null infinity, so that  $\mathcal{H} = J^+(\mathfrak{S}_{\text{right}}^-)$ .

### 6.1.3 Black hole, non-physical

The “non-physical” acoustic black hole, because it does possess an infinite velocity singularity in the fluid flow, now does have the potential of containing a curvature singularity in the spacetime geometry. Indeed, inspection of the Penrose–Carter diagram in figure 26 confirms the presence of a spacelike singularity.

### 6.1.4 Extremal black hole

The global causal structure of the extremal acoustic black hole, as represented in figure 27, is rather similar (but not identical) to that for a generic acoustic black hole. It is also identical to the causal structure of the critical black hole considered below. Differently from gravitational black holes, the major differences between extremal and non-extremal configurations are in this case geometrical rather than topological. In this sense the extremal limit for acoustic spacetimes appears to be better behaved than that for general relativistic spacetimes. Actually the absence of topological features of extremal spacetimes in acoustic geometries can be regarded as another evidence of the fact that in acoustic geometries the conceptual degeneracies of general relativity are often solved. For instance, the Penrose–Carter diagram for the extremal black hole solution of general relativity is topologically different from that for the non-extremal case and this is indeed the origin of the possibility to formulate a third law of thermodynamics for black holes. In this case the absence of Hawking temperature seems tied up with a non-trivial change in the

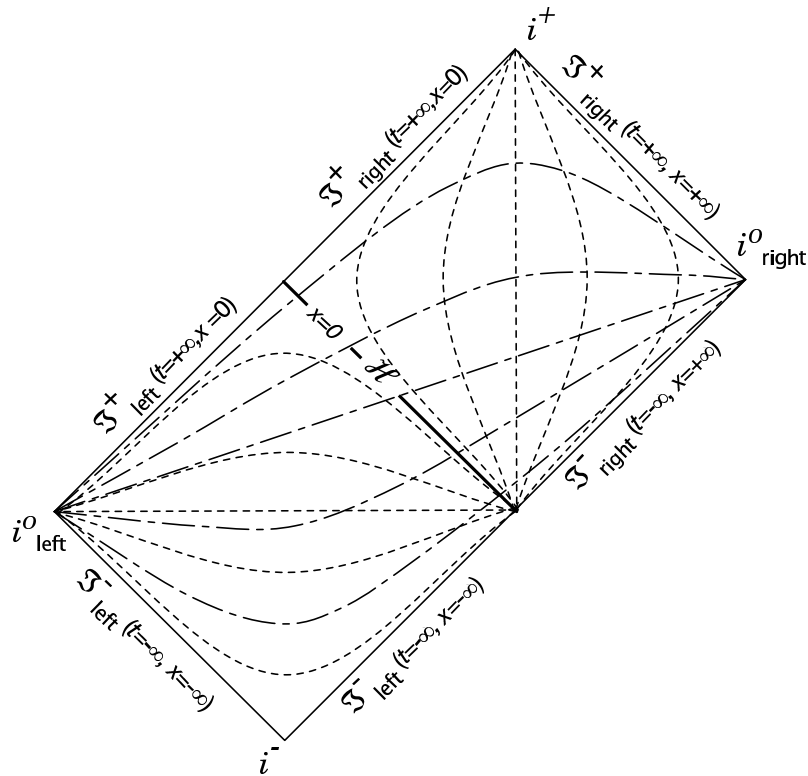


Figure 25: Conformal diagram of an acoustic white hole.

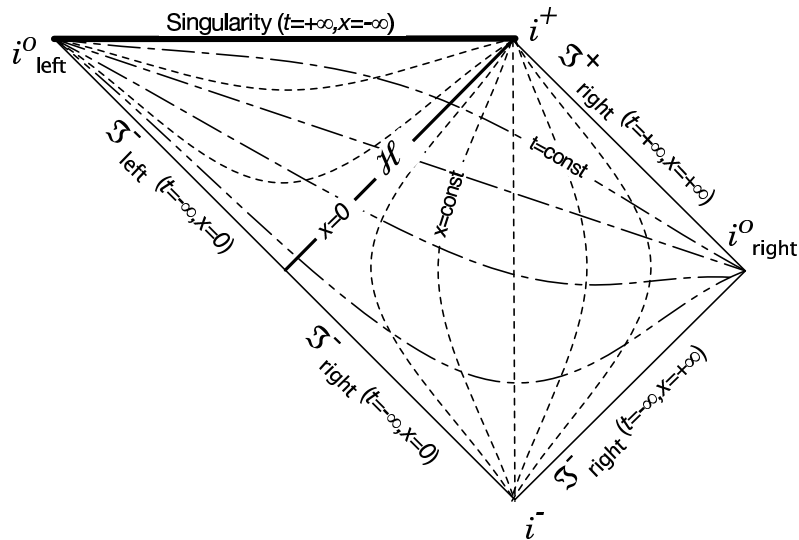


Figure 26: Conformal diagram of an unphysical acoustic black hole. The thick horizontal line corresponding to  $x = -\infty$  is a spacelike singularity.



topological structure of the spacetime with deep consequences on the black hole dynamics. However the analog acoustic spacetime is showing us that the the existence (or otherwise) of Hawking radiation is a purely kinematic feature that is independent of the dynamics underlying the evolution of the spacetime (i.e. on the Einstein equations). This is why in these acoustic geometries the temperature effects are not directly tied up with entropy considerations as in the four laws of black hole mechanics [1, 7, 8].

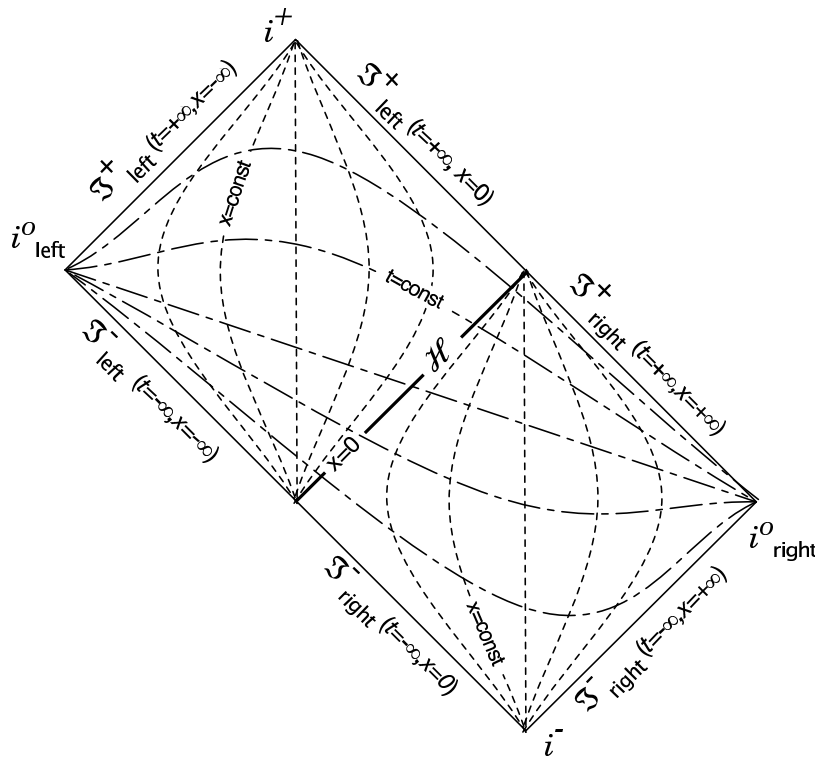


Figure 27: Conformal diagram of an acoustic extremal black hole. This is identical to the conformal diagram of an acoustic critical black hole.

### 6.1.5 Critical black hole

The critical acoustic black hole has causal structure identical to the extremal black hole, already represented in figure 27. The differences are again geometrical, not topological, and do not show up at the level of global causal structure.

## 6.2 Flows with two sonic points

### 6.2.1 Black and white hole

The acoustic geometry for a black hole–white hole combination again has no singularities in the fluid flow and no singularities in the spacetime curvature. In particular, from figure 28, we note the complete absence of singularities. Furthermore as  $x_2 \rightarrow x_1$ , so that the two horizons coalesce, the causal structure smoothly limits to that of the extremal

black hole described in figure 27 above. This behaviour is in marked contrast to what typically happens in standard general relativity, where the extremal limit is quite singular.

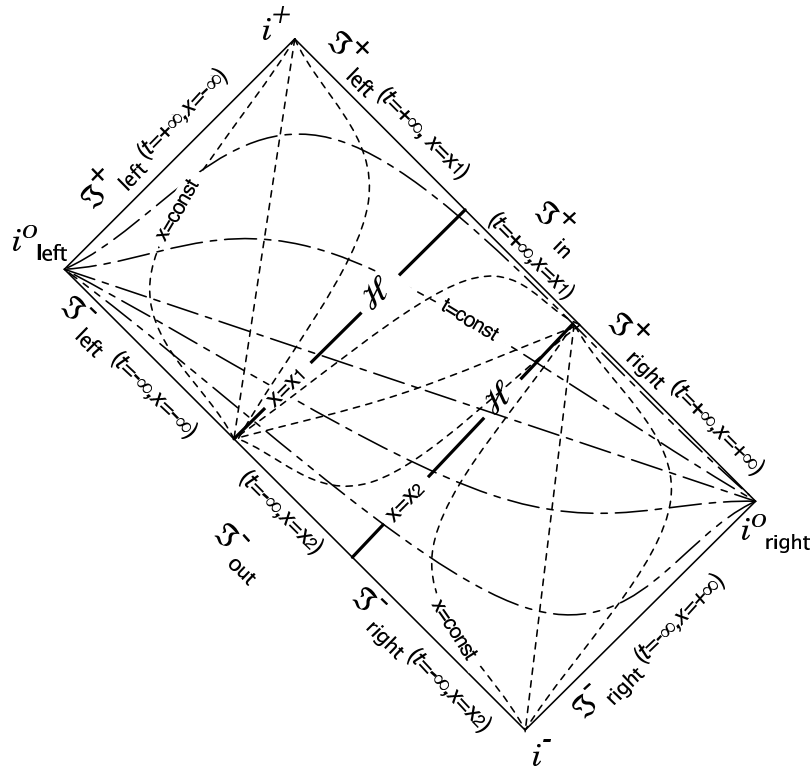


Figure 28: Conformal diagram of an acoustic black hole–white hole pair. Note the complete absence of singularities. Furthermore as  $x_2 \rightarrow x_1$  the two horizons coalesce, and the causal structure smoothly limits to that of the extremal black hole in figure 27.

### 6.2.2 Ring configuration

The ring configuration represented in figure 29 is effectively a black hole–white hole combination subject to periodic boundary conditions. As such it cannot strictly speaking be represented on a single flat piece of paper but must be drawn on a cylindrical sheet of paper. For practical purposes however a single flat sheet of paper with suitable identifications suffices.

### 6.2.3 Two black holes

For our final example of a stationary acoustic geometry we consider the case of two black hole horizons. From figure 30 we again note the complete absence of any spacetime singularity, despite the presence of two well-defined symmetrically placed event horizons.

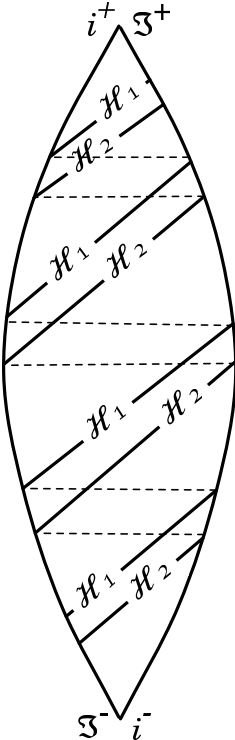


Figure 29: Ring hole: Conformal diagram of an acoustic black hole–white hole pair in a ring.

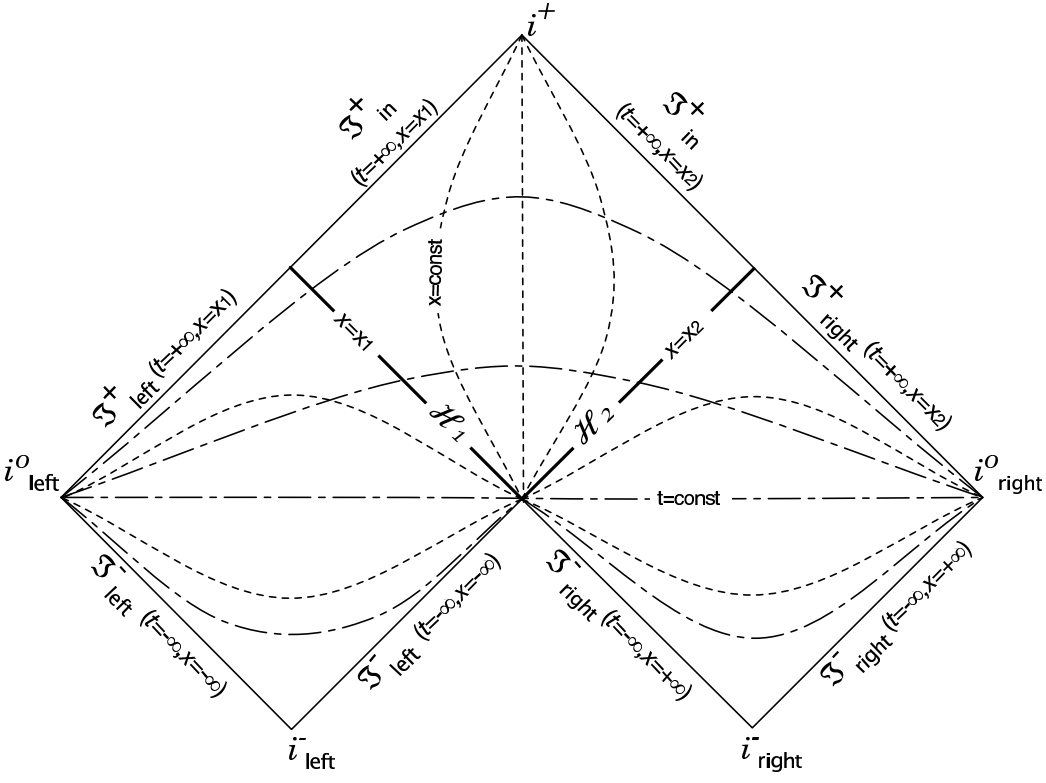


Figure 30: Conformal diagram of a flux with two acoustic black holes.

## 7 Compactification — Dynamical geometries

Let us now consider the Penrose–Carter diagrams for the global causal structure of time-dependent acoustic geometries. In all the cases considered below the geometry is trivial in the infinite past (flat Minkowski space), but has some nontrivial causal structure in the infinite future, with the concomitant presence of one or more event horizons.

### 7.1 Flows developing one sonic point

#### 7.1.1 Black hole

Formation of an acoustic black hole by switching on a fluid flow is represented in figure 31. This is the analogue, in the acoustic geometries, of an astrophysical black hole formed by stellar collapse.

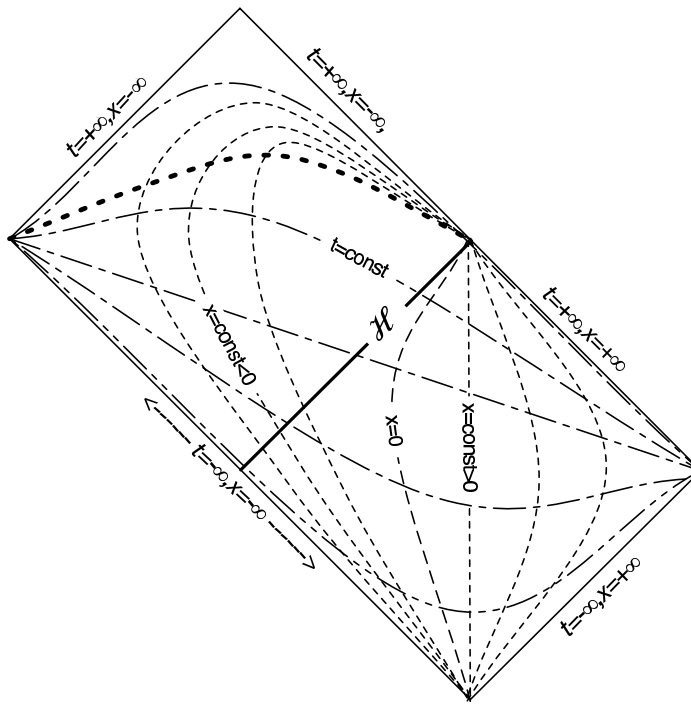


Figure 31: Conformal diagram of the switching on of an acoustic black hole. Note that the lines  $x = \text{const}$  become null at the apparent horizon (dashed line).

#### 7.1.2 White hole

In figure 32 we present the Penrose–Carter diagram of a white hole that is switched on as the fluid flow is accelerated from zero to its final partially supersonic flow.

#### 7.1.3 Black hole, non-physical

For this geometry, represented by figure 33, there is a region of infinite velocity flow at left spatial infinity ( $x \rightarrow -\infty$ ) for all finite times. This indicates the existence of a spacetime

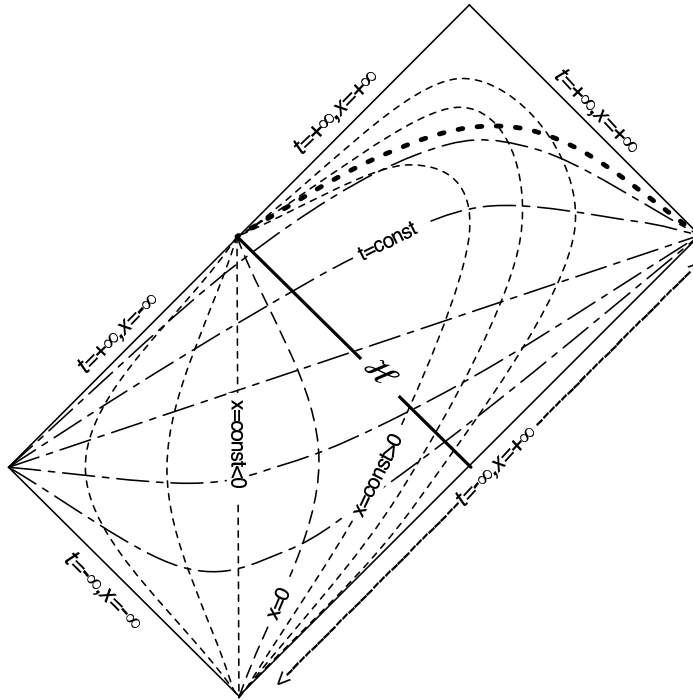


Figure 32: Conformal diagram of the formation of an acoustic white hole.

singularity that reaches back asymptotically to the infinite past.

#### 7.1.4 Extremal black hole

In figure 34 we present the Penrose–Carter diagram for the causal structure of an extremal black hole that is switched on as a fluid flow is accelerated from zero velocity to exactly reach the speed of sound. Note the strong resemblance to the case of switching on a single black hole, even though in this case the apparent horizon is a single point at future infinity.

#### 7.1.5 Critical black hole

The qualitative features of the Penrose–Carter diagram for the formation of a critical black hole are actually identical to that for formation of an extremal black hole, as presented in figure 34. The differences lie in the details of the spacetime geometry, but global causal structures are identical.

## 7.2 Flows developing two sonic points

By now the general pattern of the results should be clear. Adding time dependence so that we can explicitly discuss black hole formation in these acoustic geometries has complicated the spacetime geometry but has not led to massive modifications of the qualitative causal structure.

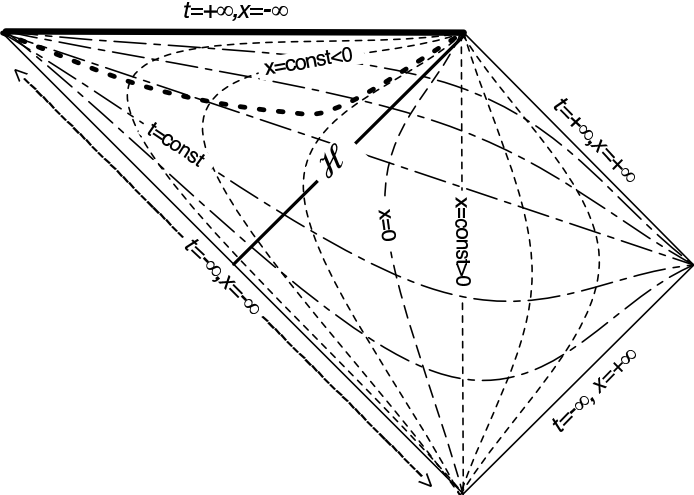


Figure 33: Conformal diagram of the formation of an unphysical acoustic black hole.

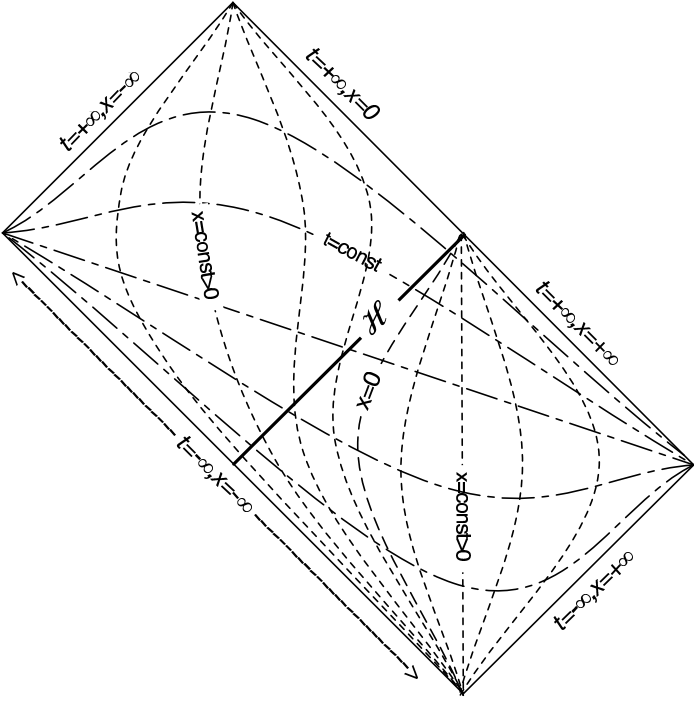


Figure 34: Conformal diagram of the formation of an acoustic extremal black hole. The causal structure is identical to that for the formation of an acoustic critical black hole.

### 7.2.1 Black and white hole

When a black hole–white hole pair is formed, as in figure 35, the major change compared to an eternal black hole–white hole pair lies in the behaviour of the apparent horizon.

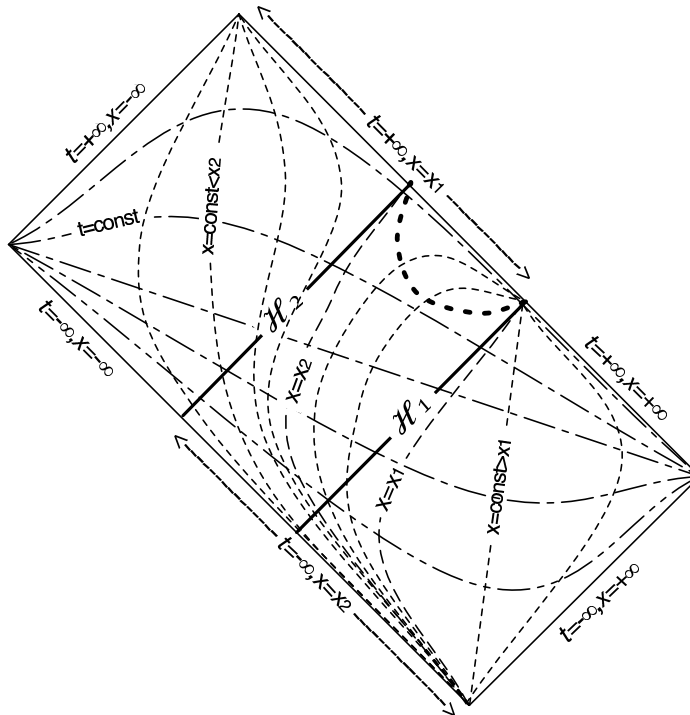


Figure 35: Conformal diagram of the formation of an acoustic black hole–white hole pair.

### 7.2.2 Ring geometry

Switching on a black hole/white hole combination in the ring geometry generates the causal structure presented in figures 36 and 37.

### 7.2.3 Two black holes

The switching on of paired black holes produces the pleasingly symmetric Penrose–Carter diagram of figure 38. Note the complete absence of any singularities and the presence of a bifurcation point where the two horizons intersect. This spacetime is not time reversal invariant, and serves as an explicit counterexample to the mistaken idea that a bifurcate horizon is necessarily Killing.



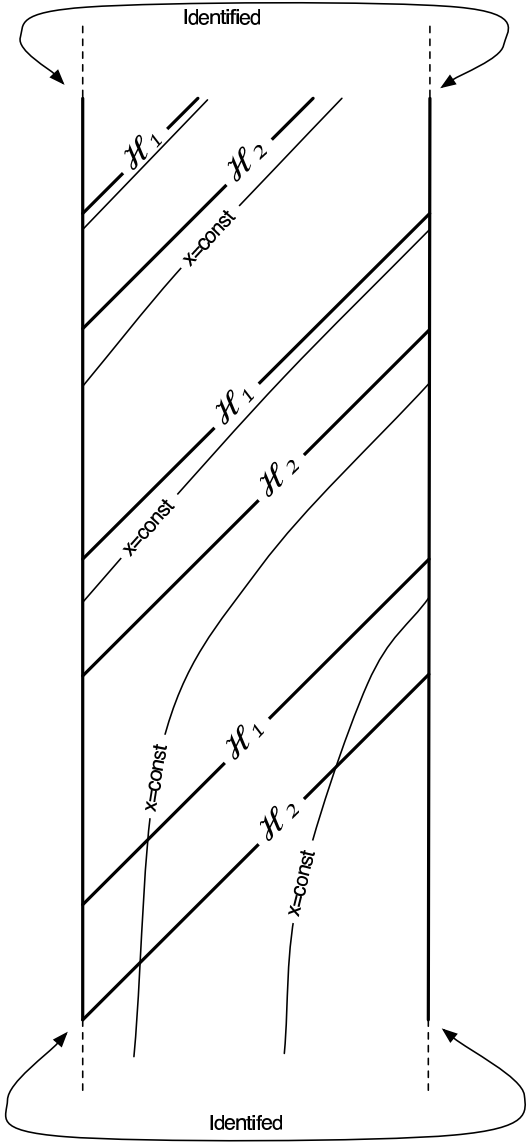


Figure 36: Diagram of the formation of an acoustic black hole/white hole pair in a ring, before compactification.

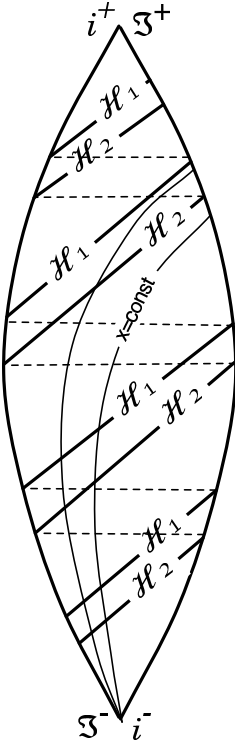


Figure 37: Conformal diagram of the formation of an acoustic black hole/white hole pair in a ring.

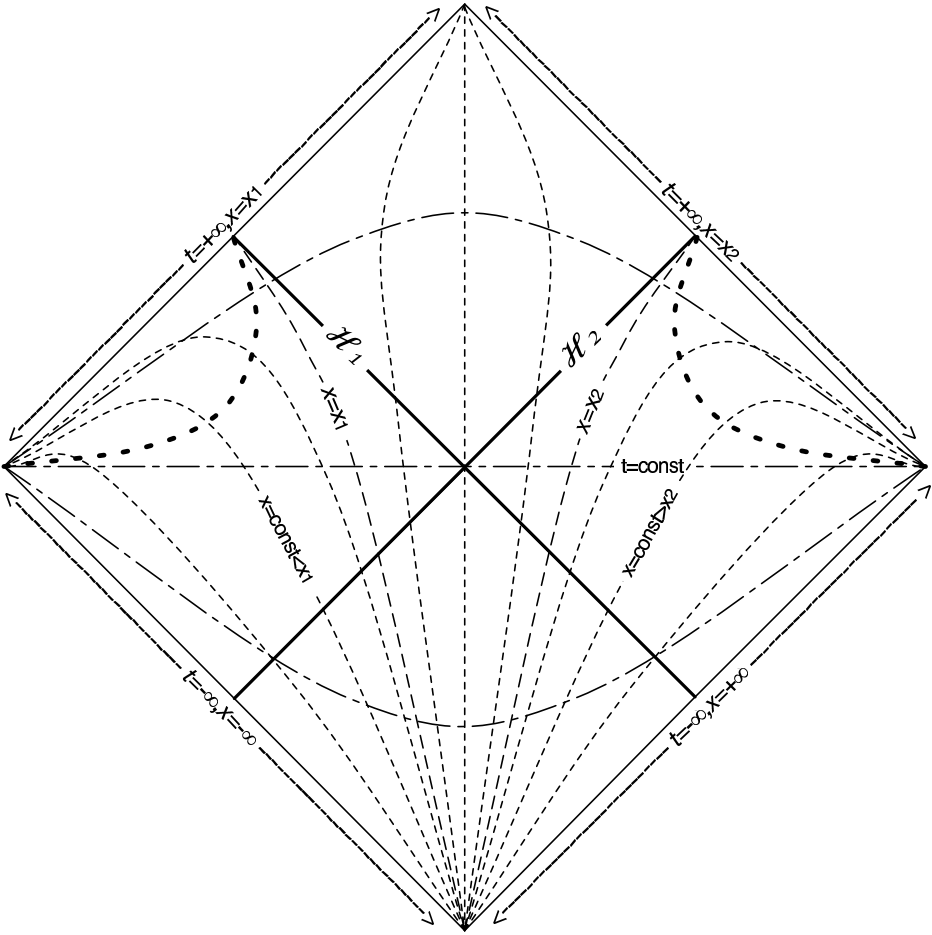


Figure 38: Conformal diagram of the generation of a fluid flow with two acoustic black holes.

## 8 Analytic extension

After describing the causal structures for our catalog of acoustic spacetimes, we will now pass to discuss the mathematical possibility of extending these geometries beyond their boundaries. As we commented in section 2, when one analyses physical acoustics in 2+1 and 3+1 dimensions (from which our 1+1 geometries follow by reduction), one arrives at a specific acoustic metric and not to an equivalence class of conformally related metrics. This is the point of view we adopt in this section. In particular, the following discussion assumes an acoustic metric of the form (3.3) with constant  $c$ . For example, the acoustic metric that one naturally finds for a barotropic fluid in 3+1 dimensions is (3.3) multiplied by a specific conformal factor  $\Omega^2 = \rho(c)/c$ , that in the simplest case in which  $c = \text{constant}$  becomes constant and so irrelevant<sup>5</sup>.

In general relativity, the standard way to show that a horizon is a perfectly regular region of spacetime, is to rewrite the metric in coordinates that are regular at the horizon, as we did at the beginning of section 6 [24, 25, 28]. With the same line of reasoning we can see that the geometry described by the metric (2.10) can be mathematically extended beyond the range described by the physical coordinates  $t$  and  $x$ . Look for example at the conformal diagram of the white hole acoustic spacetime, presented in figure 25. In this particular acoustic geometry, there are geodesics starting from any event inside the diagram that can reach  $\mathfrak{S}_{\text{left}}^+$  (the upper diagonal line  $t = +\infty, x = 0$ ), within a finite lapse of their affine parameter (see the Appendix for a proof), so the spacetime is geodesically incomplete. This feature, together with the regularity of this region, implies that the white hole geometry can be mathematically extended beyond its open boundary in the future. If one requires the extension to be made analytically, then it is not difficult to see that the maximally extended spacetime would be the one represented by the conformal diagram in figure 39. In that diagram, the white hole geometry is supplemented with a black-hole geometry to give rise to an inextensible metric manifold. This discussion, or minor variations of it, applies to most of the acoustic metrics described in this paper. Given a conformal diagram, the reader will not find it difficult to construct its maximal analytic extension.

Of course, the extended part of the diagram (the black hole part in our example), does not exist in physical space and time. It is somewhat like another parallel world. From the point of view of observers in the laboratory any discussion about this parallel world does not make much sense. This is because the connection between the two worlds happens at an infinite amount of laboratory time in the future. However, for internal observers (hypothetical observers whose internal structure is governed by an exchange of virtual phonons, and who therefore react directly to the acoustic metric as the physical metric) this connection happens at a finite amount of proper time; and so, for them it makes perfectly good mathematical sense to ask whether there is something beyond this boundary. In other words: If a signal is sent from the asymptotic region on the right towards the left (against the flow), observers in the laboratory will say that the signal never reaches the sonic point at  $x = 0$ . In contrast, the internal observers will believe that by swimming against the flow they should be able to reach  $x = 0$  in a finite amount of

---

<sup>5</sup>Actually, in 1+1 dimensions the continuity equation gives  $\rho v = \text{const}$  so that  $\rho(v) \propto 1/v$  is not constant (although at least it is finite at the sonic points). In contrast, in 3+1 dimensions with appropriate symmetry (such as a 1-dimensional duct with variable cross sections) we certainly can arrange  $c = \text{constant}$ .



their proper time, and so they should also be able to experience what happens once they cross that point. However, the fact that  $x = 0$  can be reached in a finite lapse of proper time, as opposed to the infinite amount of laboratory time  $t$ , is not due to an unfortunate choice of the  $t$  coordinate, but rather to a dynamical slowing down of the clocks carried by the internal observers as the sonic point is approached.<sup>6</sup> Hence, the internal observers will actually be hibernating near the sonic point, and will remain there forever from our laboratory point of view.

There is another important issue of physics hiding in the mathematics of maximal analytic extension. While there is no doubt that maximal analytic extension can successfully be carried out as a mathematical exercise, one should also think about the physics of the approximations being made. We have already made clear that maximal analytic extension only appears to make sense for hypothetical internal observers that couple only to the acoustic metric (2.10), and do not see the physical spacetime metric of special relativity. But this is at best a low-energy approximation; at high enough energy the atomic nature of matter comes into play and ultimately phonon dispersion relations turn over [13], destroying the acoustic approximation. Indeed the physically-motivated breakdown of the notion of maximal analytical extension due to the high-energy breakdown of the relativistic approximation seems to be a general feature of analog spacetimes. For example, this also shows up in analog models based on fermionic quasi-particles in  $^3\text{He-A}$  as noticed in [35, 36].<sup>7</sup>

In contrast, in standard general relativity with a single unique physical metric and strict adherence to the Einstein Equivalence Principle, the absence of such problems related to maximal analytic extension is automatic. In multi-metric theories, or indeed any theory that does not impose strict adherence to the Einstein Equivalence Principle, we may find that the process of maximal analytic extension fails for physical (rather than mathematical) reasons.

If one takes the view (which is *not* standard within the general relativity community) that Einstein gravity is simply a low-energy approximation to some radically different and more fundamental theory of quantum gravity, then this observation based on the analogue models suggests that there might similarly be physical problems with maximal analytic extension in real physical spacetimes, not because there is anything wrong with the mathematics of maximal analytic extension, but because the physical hypotheses and approximations underlying the use of differential geometry and the mathematical machinery of manifolds may break down at the locations where analytic extension seems mathematically natural.

Within the context of the acoustic geometries, this physical breakdown in the pro-

---

<sup>6</sup>Consider for example a “sound clock,” constructed by letting a sound pulse bounce between two points separated by a constant distance  $d$  along a direction orthogonal to the flow in the pipe. For such a clock located at a given value of  $x$ , the round-trip time (as measured in the laboratory) is  $T(x) = 2d/C(x)$ , where  $C(x)$  is the pulse speed with respect to the laboratory. The latter is easily found by requiring that in the frame comoving with the fluid the pulse speed be still  $c$ , so  $C(x) = (c^2 - v(x)^2)^{1/2}$  and

$$T(x) = \frac{2d}{c} (1 - v(x)^2/c^2)^{-1/2} .$$

If the internal observers use  $T(x)$  as their standard of time, it is immediate to account for the relation between  $t$  and their proper time, as predicted by the metric (2.10).

<sup>7</sup>Those authors also consider Carter–Penrose diagrams for that specific model, obtaining similar but not identical causal structures.

cess of analytic extension is in a sense obvious — but we submit that without having a concrete physical example of this process at hand it would be difficult to see why the mathematically well-defined process of analytic extension should be viewed with some circumspection for physics reasons. In particular, note that the arguments we have used in order to exclude the possibility, for the internal observers, of “crossing the boundary at  $t = +\infty$ ,” rely on the existence of a privileged external structure — the laboratory. Without it, from the perspective offered by the metric (2.10) alone, we could not discard the possibility for the parallel world beyond  $t = +\infty$  to exist.

## 9 Summary and conclusions

Many properties of acoustics in moving fluids can be understood by recourse to the tools and notions that appear in the study of fields and rays in effective spacetime geometries. On the other hand, the analogue gravity programme [6, 9, 29, 30, 31, 32, 33, 34] also aims to shed light on different problems of the physics of fields in curved spacetime backgrounds by analyzing acoustic systems (more generally, condensed matter systems) with similar “effective” geometrical properties. In particular, in this paper our interest have been centered on (1+1)-dimensional background geometries containing sonic horizons, either present since the beginning of time or with apparent horizons being created at a certain moment. We have produced a rather complete catalogue of 1+1 acoustic spacetimes taking into account their naturalness as models of acoustic effective manifolds in a condensed matter laboratory. The specific characteristics of each of these spacetimes will have important consequences regarding vacuum polarization effects. We will analyze this issue in a follow-up paper.

We have separated the different geometries into subclasses, depending on the existence of either one or two sonic points, and to their eternal or dynamical character. Then, we have chosen specific velocity profiles (that is, specific 1+1 spacetime geometries), in such a way that they are easy-to-manipulate representatives of each subclass. Using these profiles, we have calculated the form of the null coordinates  $u$  and  $w$  as a function of the laboratory coordinates  $t$  and  $x$ . In this way, we have described the behaviour of null rays (geometric acoustics) in each of these geometries.

In this paper we have been primarily interested in the global causal structures of these acoustic manifolds. Two metrics differing only by a conformal factor share the same causal structure. Therefore, to describe the causal structures of our catalogue of acoustic spacetimes we have constructed their conformal diagrams.

Finally, by looking at the conformal diagram of a white hole spacetime (we have taken this particular spacetime as a simple and illustrative example), we have discussed the different views that one could have regarding the extendibility of that geometry, depending on whether one views the situation as an internal or an external (laboratory) observer. An observer in the laboratory will be reluctant to think about anything existing beyond its space and time, whereas for a hypothetical internal observer, whose analysis of the world is performed only through acoustic experiments, the notion of maximal analytic extension would seem to make perfectly good sense. However once we take note of the fact that acoustics in general is only a low-energy approximation to more fundamental underlying physics, we see that analytic extension, while perfectly good mathematics, is physically dubious. This *might* have implications for real physical gravity if one adopts

the perhaps unpopular viewpoint that what we know as Einstein gravity (and in particular the approximations underlying the use of manifolds and differential geometry) are only low-energy manifestations of some radically different underlying theory.

## Appendix: Geodesic incompleteness

Let us prove that any acoustic spacetime  $(\mathcal{M}, g)$ , as defined in section 2, which is associated with a flow that contains sonic points, is geodesically incomplete. We shall show this by arguing that the affine parameter along a geodesic attains a finite value as a sonic point is approached. This is true for timelike and spacelike geodesics (for which the affine parameter is simply proportional to proper length along the curve), as well as for null geodesics. For the sake of definiteness, we shall restrict ourselves to a stationary situation, and we shall focus on the case in which the sonic point corresponds to the asymptotic line  $u = +\infty$ . Furthermore, we shall assume that  $x_S = 0$ . Other cases can be easily dealt with in a similar way.

If  $\lambda$  is an affine parameter, the geodesic equation is

$$\frac{d^2 x^a}{d\lambda^2} + \Gamma^a_{bc} \frac{dx^b}{d\lambda} \frac{dx^c}{d\lambda} = 0. \quad (\text{A.1})$$

It is convenient to work in null coordinates. Then it will be enough to consider the equation

$$\frac{d^2 u}{d\lambda^2} + \Gamma^u_{bc} \frac{dx^b}{d\lambda} \frac{dx^c}{d\lambda} = 0. \quad (\text{A.2})$$

Since the only non-vanishing Christoffel coefficient of the type  $\Gamma^u_{bc}$  is  $\Gamma^u_{uu}$ , this equation becomes

$$\frac{d^2 u}{d\lambda^2} + \Gamma^u_{uu} \left( \frac{du}{d\lambda} \right)^2 = 0, \quad (\text{A.3})$$

with

$$\Gamma^u_{uu} = g^{uw} \frac{\partial g_{uw}}{\partial u} = \frac{\partial}{\partial u} \ln |g_{uw}| = \frac{\partial}{\partial u} \ln \left( \Omega^2 |c^2 - v^2| \right), \quad (\text{A.4})$$

where the metric (3.3) with  $F = G = 1$  has been used. For our purpose, we need only know the asymptotic form of  $\lambda(u)$  as  $u \rightarrow +\infty$ . We can then use equation (3.4) in order to write, asymptotically,

$$|c^2 - v^2| \sim 2c\kappa|x| \quad (\text{A.5})$$

and

$$\Gamma^u_{uu} \sim \frac{\partial \ln |x|}{\partial u} + \frac{2}{\Omega} \frac{\partial \Omega}{\partial u}. \quad (\text{A.6})$$

If we assume that  $\Omega$  tends to a finite value at the sonic point (a very plausible hypothesis, given that it will usually be some function of density), we can ignore the last term and simply write

$$\Gamma^u_{uu} \sim \frac{\partial \ln |x|}{\partial u}. \quad (\text{A.7})$$

Since  $\ln |x| \sim \kappa(w - u)$  by equation (3.6), we find  $\Gamma^u_{uu} \sim -\kappa$ . Then equation (A.3) implies

$$\lambda \sim A - B e^{-\kappa u}, \quad (\text{A.8})$$

with  $A$  and  $B$  arbitrary constants. For  $u \rightarrow +\infty$ , the affine parameter  $\lambda$  attains a finite value.



## Acknowledgements

The research of Carlos Barceló is supported by the Education Council of the Junta de Andalucía (Spain). Matt Visser is supported by a Marsden grant administered by the Royal Society of New Zealand.

## References

- [1] W. G. Unruh, “Experimental black hole evaporation,” *Phys. Rev. Lett.* **46**, 1351–1353 (1981).
- [2] T. Jacobson, “Black hole evaporation and ultrashort distances,” *Phys. Rev. D* **44**, 1731–1739 (1991).  
T. A. Jacobson, “Introduction to black hole microscopy,” arXiv:hep-th/9510026.  
T. Jacobson, “On the origin of the outgoing black hole modes,” *Phys. Rev. D* **53**, 7082–7088 (1996) [arXiv:hep-th/9601064].  
S. Corley and T. Jacobson, “Hawking spectrum and high frequency dispersion,” *Phys. Rev. D* **54**, 1568–1586 (1996) [arXiv:hep-th/9601073].
- [3] M. Visser, “Acoustic propagation in fluids: An unexpected example of Lorentzian geometry,” arXiv:gr-qc/9311028.
- [4] W. G. Unruh, “Dumb holes and the effects of high frequencies on black hole evaporation,” *Phys. Rev. D* **51**, 2827–2838 (1995) [arXiv:gr-qc/9409008].
- [5] M. Visser, “Acoustic black holes: Horizons, ergospheres, and Hawking radiation,” *Class. Quantum Grav.* **15**, 1767–1791 (1998) [arXiv:gr-qc/9712010].
- [6] M. Novello, M. Visser and G. Volovik (editors), *Artificial Black Holes* (World Scientific, Singapore, 2002).
- [7] M. Visser, “Hawking radiation without black hole entropy,” *Phys. Rev. Lett.* **80**, 3436–3439 (1998) [arXiv:gr-qc/9712016].
- [8] M. Visser, “Essential and inessential features of Hawking radiation,” *Int. J. Mod. Phys. D* **12**, 649–661 (2003) [arXiv:hep-th/0106111].
- [9] C. Barceló, S. Liberati and M. Visser, “Analog gravity from field theory normal modes?” *Class. Quant. Grav.* **18**, 3595–3610 (2001) [arXiv:gr-qc/0104001].
- [10] S. E. Perez Bergliaffa, K. Hibberd, M. Stone and M. Visser, “Wave equation for sound in fluids with vorticity,” *Physica D* **191**, 121–136 (2004) [arXiv:cond-mat/0106255].
- [11] J. W. Milnor, *Topology from the Differentiable Viewpoint* (Charlottesville, University Press of Virginia, 1965), pp. 55–57.
- [12] S. Liberati, S. Sonego and M. Visser, “Faster-than-c signals, special relativity, and causality,” *Ann. Phys. (N.Y.)* **298**, 167–185 (2002) [arXiv:gr-qc/0107091].
- [13] M. Visser, C. Barceló and S. Liberati, “Acoustics in Bose-Einstein condensates as an example of broken Lorentz symmetry,” arXiv:hep-th/0109033.

- [14] T. S. Shankara and K. K. Nandi, “Transformation of coordinates associated with linearized supersonic motion,” *J. Appl. Phys.* **49**, 5783–5789 (1978).
- [15] S. Liberati, S. Sonego and M. Visser, “Unexpectedly large surface gravities for acoustic horizons?” *Class. Quant. Grav.* **17** 2903–2923 (2000) [arXiv:gr-qc/0003105].
- [16] P. Painlevé, “La mécanique classique et la théorie de la relativité,” *C. R. Acad. Sci. (Paris)* **173**, 677–680 (1921).  
A. Gullstrand, “Allgemeine Lösung des statischen Einkörperproblems in der Einsteinschen Gravitationstheorie,” *Ark. Mat. Astron. Fys.* **16**, 1–15 (1922).
- [17] S. Kristiansson, S. Sonego and M. A. Abramowicz, *Gen. Rel. Grav.* **30**, 275–288 (1998).  
S. Sonego, J. Almergren and M. A. Abramowicz, *Phys. Rev. D* **62**, 064010 (2000) [arXiv:gr-qc/0005106].
- [18] G. E. Volovik, “What can the quantum liquid say on the brane black hole, the entropy of extremal black hole and the vacuum energy?” *Found. Phys.* **33**, 349–368 (2003) [arXiv:gr-qc/0301043].
- [19] M. Visser, “Heuristic approach to the Schwarzschild geometry,” arXiv:gr-qc/0309072.
- [20] L. J. Garay, J. R. Anglin, J. I. Cirac and P. Zoller, “Black holes in Bose-Einstein condensates,” *Phys. Rev. Lett.* **85**, 4643–4647 (2000) [arXiv:gr-qc/0002015].
- [21] L. J. Garay, J. R. Anglin, J. I. Cirac and P. Zoller, “Sonic black holes in dilute Bose-Einstein condensates,” *Phys. Rev. A* **63**, 023611 (2001) [arXiv:gr-qc/0005131].
- [22] C. Barceló, S. Liberati and M. Visser, “Towards the observation of Hawking radiation in Bose-Einstein condensates,” *Int. J. Mod. Phys. A* **18**, 3735–3745 (2003) [arXiv:gr-qc/0110036].
- [23] S. W. Hawking, “The event horizon,” in *Black Holes*, edited by C. DeWitt and B. S. DeWitt (New York, Gordon and Breach, 1973), pp. 1–55. Reissued in S. Hawking, *Hawking on the Big Bang and Black Holes*, edited by C. DeWitt and B. S. DeWitt (Singapore, World Scientific, 1993), pp. 27–74.
- [24] C. W. Misner, K. S. Thorne and J. A. Wheeler, *Gravitation* (New York, Freeman, 1973).
- [25] S. W. Hawking and G. F. R. Ellis, *The Large Scale Structure of Space-Time* (Cambridge, Cambridge University Press, 1973).
- [26] K. S. Thorne, R. H. Price and D. A. MacDonald (editors), *Black Holes: The Membrane Paradigm* (Yale University Press, 1986), pp. 213–215.
- [27] R. Penrose, “Conformal treatment of infinity,” in *Relativity, Groups and Topology*, (Gordon and Breach Science Publisher, New York, 1964).  
B. Carter, “Complete analytic extension of the symmetry axis of Kerr’s solution of Einstein’s equations,” *Phys. Rev.* **141**, 1242–1247 (1966).
- [28] R. M. Wald, *General Relativity* (Chicago, University of Chicago Press, 1984).
- [29] U. R. Fischer and G. E. Volovik, “Thermal quasi-equilibrium states across Landau horizons in the effective gravity of superfluids,” *Int. J. Mod. Phys. D* **10**, 57–88 (2001) [arXiv:gr-qc/0003017].

- U. R. Fischer and M. Visser, “Riemannian geometry of irrotational vortex acoustics,” *Phys. Rev. Lett.* **88**, 110201 (2002) [arXiv:cond-mat/0110211].
- U. R. Fischer and M. Visser, “On the space-time curvature experienced by quasiparticle excitations in the Painlevé–Gullstrand effective geometry,” *Ann. Phys. (N.Y.)* **304**, 22–39 (2003) [arXiv:cond-mat/0205139].
- U. R. Fischer and M. Visser, “Warped space-time for phonons moving in a perfect nonrelativistic fluid,” *Europhys. Lett.* **62**, 1–7 (2003) [arXiv:gr-qc/0211029].
- P. O. Fedichev and U. R. Fischer, “‘Cosmological’ particle production in oscillating ultracold Bose gases: The role of dimensionality,” arXiv:cond-mat/0303063.
- P. O. Fedichev and U. R. Fischer, “Hawking radiation from sonic de Sitter horizons in expanding Bose-Einstein-condensed gases,” *Phys. Rev. Lett.* **91**, 240407 (2003) [arXiv:cond-mat/0304342].
- P. O. Fedichev and U. R. Fischer, “Observing quantum radiation from acoustic horizons in linearly expanding cigar-shaped Bose-Einstein condensates,” *Phys. Rev. D* **69**, 064021 (2004) [arXiv:cond-mat/0307200].
- U. R. Fischer, “Quasiparticle universes in Bose-Einstein condensates,” arXiv:cond-mat/0406086.
- [30] C. Barceló, S. Liberati and M. Visser, “Analog gravity from Bose-Einstein condensates,” *Class. Quantum Grav.* **18**, 1137–1156 (2001) [arXiv:gr-qc/0011026].
- [31] S. E. C. Weinfurtner, “Simulation of gravitational objects in Bose-Einstein condensates” (in German), arXiv:gr-qc/0404022.
- [32] S. E. C. Weinfurtner, “Analog model for an expanding universe,” arXiv:gr-qc/0404063.
- [33] C. Barceló, S. Liberati and M. Visser, “Analogue models for FRW cosmologies,” *Int. J. Mod. Phys. D* **12**, 1641–1650 (2003) [arXiv:gr-qc/0305061].
- [34] C. Barceló, S. Liberati and M. Visser, “Probing semiclassical analogue gravity in Bose-Einstein condensates with widely tunable interactions,” *Phys. Rev. A* **68**, 053613 (2003) [arXiv:cond-mat/0307491].
- [35] T. A. Jacobson and G. E. Volovik, “Effective spacetime and Hawking radiation from moving domain wall in thin film of He-3-A,” *Pisma Zh. Eksp. Teor. Fiz.* **68**, 833–838 (1998) [*JETP Lett.* **68**, 874–880 (1998)] [arXiv:gr-qc/9811014].
- [36] T. Jacobson and T. Koike, “Black hole and baby universe in a thin film of He-3-A”. Published in *Artificial Black Holes* Ed. M. Novello, M. Visser and G. Volovik, (World Scientific, Singapore, 2002) [arXiv:cond-mat/0205174].